Title

Tetramethylpyrazine: A promising drug for the treatment of pulmonary hypertension

Authors

Chen, Yuqin
Lu, Wenju
Yang, Kai
et al.

Peer reviewed

RESEARCH PAPER

Tetramethylpyrazine: A promising drug for the treatment of pulmonary hypertension

Yuqin Chen[1] | Wenju Lu[1] | Kai Yang[1] | Xin Duan[4] | Mengxi Li[1] | Xiuqing Chen[1] | Jie Zhang[1] | Meidan Kuang[1] | Shiyun Liu[1] | Xiongting Wu[1] | Guofa Zou[1] | Chunli Liu[1] | Cheng Hong[1] | Wenjun He[1] | Jing Liao[1] | Chi Hou[5] | Zhe Zhang[1] | Qiuyu Zheng[1] | Jiyuan Chen[1] | Nuofu Zhang[1] | Haiyang Tang[1,2] | Rebecca R. Vanderpool[2] | Ankit A. Desai[2] | Franz Rischard[2] | Stephen M. Black[2] | Joe G.N. Garcia[2] | Ayako Makino[6] | Jason X.-J. Yuan[6] | Nanshan Zhong[1] | Jian Wang[1,3,6]

[1]State Key Laboratory of Respiratory Disease, National Clinical Research Center for Respiratory Disease, Guangdong Key Laboratory of Vascular Disease, Guangzhou Institute of Respiratory Health, The First Affiliated Hospital of Guangzhou Medical University, Guangzhou, China

[2]Departments of Medicine and Physiology, The University of Arizona, Tucson, Arizona

[3]Division of Pulmonary and Critical Care Medicine, The People's Hospital of Inner Mongolia, Huhhot, China

[4]State Key Laboratory of Cardiovascular Disease, Department of Cardiology, Fuwai Hospital, National Center for Cardiovascular Disease, Chinese Academy of Medical Sciences and Peking Union Medical College, Beijing, China

[5]Department of Neurology, Guangzhou Women and Children's Medical Center, Guangzhou, China

[6]Department of Medicine, University of California, San Diego, La Jolla, California, USA

Correspondence

Jian Wang, State Key Laboratory of Respiratory Diseases, Guangzhou Institute of Respiratory Health, The First Affiliated Hospital of Guangzhou Medical University,

Background and Purpose: Tetramethylpyrazine (TMP) was originally isolated from the traditional Chinese herb ligusticum and the fermented Japanese food natto and has since been synthesized. TMP has a long history of beneficial effects in the treatment of many cardiovascular diseases. Here we have evaluated the therapeutic effects of TMP on pulmonary hypertension (PH) in animal models and in patients with pulmonary arterial hypertension (PAH) or chronic thromboembolic pulmonary hypertension (CTEPH).

Experimental Approach: Three well-defined models of PH -chronic hypoxia (10% O_2)-induced PH (HPH), monocrotaline-induced PH (MCT-PH) and Sugen 5416/hypoxia-induced PH (SuHx-PH) - were used in Sprague-Dawley rats, and assessed by echocardiography, along with haemodynamic and histological techniques. Primary cultures of rat distal pulmonary arterial smooth muscle cells (PASMCs) were used to study intracellular calcium levels. Western blots and RT-qPCR assays were also used. In the clinical cohort, patients with PAH or CTEPH were recruited. The effects of TMP were evaluated in all systems.

Key Results: TMP (100 mg·kg^{-1}·day^{-1}) prevented rats from developing experimental PH and ameliorated three models of established PH: HPH, MCT-PH and SuHx-PH. The therapeutic effects of TMP were accompanied by inhibition of intracellular calcium homeostasis in PASMCs. In a small cohort of patients with PAH or CTEPH, oral

151 Yanjiang Road, Guangzhou, Guangdong 510120, China.
Email: jiw037@ucsd.edu

administration of TMP (100 mg, t.i.d. for 16 weeks) increased the 6-min walk distance and improved the 1-min heart rate recovery.

Conclusion and Implications: Our results suggest that TMP is a novel and inexpensive medication for treatment of PH. Clinical trial is registered with www.chictr.org.cn (ChiCTR-IPR-14005379).

1 | INTRODUCTION

Pulmonary arterial hypertension (PAH) is a progressive disease associated with a high mortality. Sustained pulmonary vasoconstriction at the early stage and excessive pulmonary vascular remodelling in the late stage are two major causes of the elevated pulmonary vascular resistance (PVR) and pulmonary arterial pressure (PAP) in patients with PAH and experimental animal models of pulmonary hypertension PH). Although progress has been made in our understanding of the molecular mechanism and disease management, the prognosis of PAH is still poor, with a 1-year survival rate of 91% (Benza et al., 2010; Hao et al., 2014) and a 3-year survival rate of 80% or less, (Clements et al., 2012; Hao et al., 2014; Kane et al., 2011; Thenappan, Glassner, & Gomberg-Maitland, 2012). For decades, treatment options for PAH have been focused on agents that induce vasodilation and anticoagulation and drugs that have anti-proliferative effects on pulmonary arterial smooth muscle cells (PASMCs) and (myo)fibroblasts (Pullamsetti et al., 2014; Robinson, Pugliese, Fox, & Badesch, 2016). New classes of therapies have been developed over the past 20 years including **prostacyclin (PGI$_2$**; epoprostenol) and its analogues (**iloprost** and **treprostinil**), **PGI$_2$ receptor (IP)** agonists, such as **selexipag, endothelin-1 (ET-1) receptor** antagonists (**ambrisentan, bosentan** and **macitentan**), PDE inhibitors (**sildenafil, tadalafil**, and treprostinil), and the latest approved **soluble GC (sGC)** stimulators (**riociguat**). Inhaled **NO** has also been used to treat paediatric and adult patients with PAH

(Benza, Mathai, & Nathan, 2017; Divakaran & Loscalzo, 2017; Frumkin, 2012; Putnam et al., 2016). While these agents can improve haemodynamics, quality of life, and functional capacity, the worldwide usage of these drugs is largely limited by their high price. In Canada, PAH medications cost between Can$881 (tadalafil) and Can$4,028 (amberisentan) per month (Coyle et al., 2016). In the United States, the cost for bosentan and epoprostenol can be as much as $25,000 and $35,000 per month, respectively (Wryobeck, Lippo, McLaughlin, Riba, & Rubenfire, 2007). According to a national survey in China, over 50% of PAH patients do not use any kind of PAH-specific therapies due to the financial burden (Zhai et al., 2017). It is thus important to develop and identify new medications that have equal or higher efficacy but are affordable, readily available, and easily administered for patients with PAH.

Tetramethylpyrazine (TMP), also known as ligustrazine, is a compound isolated from the traditional Chinese herb ligusticum (or cnidium) and the fermented Japanese food natto. TMP, which has also been synthesized, exerts vasodilative, anticoagulant, anti-inflammatory and positive inotropic effects. TMP has been widely used for the treatment of cardiovascular diseases (Guo, Liu, & Shi, 2016), due to its long history of safe usage, high efficacy, low expense, few adverse effects, and easy oral administration (Bai et al., 2014; Chen & Chen, 1992; Fu et al., 2012; Shaw, Chen, & Tsai, 2013; Wang et al., 2013; Zeng et al., 2013; Zhu, Wang, & Qin, 2009). In the present context, the beneficial effects of TMP have been shown in hypoxia-induced PH, as a pulmonary vasodilator and

What is already known

- Tetramethylpyrazine was originally isolated from the traditional Chinese herb ligusticum and has since been synthesized.
- Tetramethylpyrazine has a long history of beneficial effects in the treatment of many cardiovascular diseases.

What does this study add

- Tetramethylpyrazine effectively prevents and reverses pulmonary hypertension in different experimental rat models.

What is the clinical significance

- Tetramethylpyrazine exerts beneficial effects in patients with pulmonary arterial hypertension and chronic thromboembolic pulmonary hypertension.
- Tetramethylpyrazine is a novel potential effective treatment for pulmonary hypertension.

by normalizing the right ventricular hypertrophy and muscularization of pulmonary arterioles (Cai & Barer, 1989). The vasodilator effects of TMP have been later demonstrated (Oddoy, Bee, Emery, & Barer, 1991; Peng, Hucks, Priest, Kan, & Ward, 1996). However, the molecular mechanisms underlying the effects of TMP on PH remain largely unclear and require further elucidation.

Ca^{2+} is a key intracellular signalling element for both contraction and proliferation of vascular smooth muscle cells (Karaki et al., 1997). An increase in cytosolic free Ca^{2+} concentration ($[Ca^{2+}]_{cyt}$) in PASMCs is a major trigger for pulmonary vasoconstriction and an important stimulus for PASMC proliferation and migration, leading to concentric pulmonary vascular wall thickening. Elevation of $[Ca^{2+}]_{cyt}$ in PASMCs due to enhanced Ca^{2+} entry through voltage-dependent (VDCC), receptor-operated (ROCC), and store-operated (SOCC) Ca^{2+} channels is a critical mechanism involved in the development of PAH and hypoxia-induced PH (Lin et al., 2004; Wang et al., 2006; Ward, Robertson, & Aaronson, 2005; Weigand, Foxson, Wang, Shimoda, & Sylvester, 2005). Both in vivo and in vitro experiments have demonstrated that (a) store-operated Ca^{2+} entry (SOCE) and receptor-operated Ca^{2+} entry (ROCE) are enhanced, using TRPC and Orai channels, along with STIM, and are up-regulated in PASMCs from IPAH patients compared to cells isolated from normal subjects (Kuhr, Smith, Song, Levitan, & Yuan, 2012) and (b) chronic hypoxia enhances SOCE and ROCE as a result of up-regulation of channels involved in store-operated Ca^{2+} channel formation (Wang et al., 2005; Weigand et al., 2005). In normal rat and human PASMCs, hypoxia-enhanced

SOCE and ROCE are at least in part mediated by the hypoxia-mediated up-regulation of TRPC1/C6, Orai2, and STIM1, the main components of SOCC/ROCC in PASMCs (Fernandez et al., 2015; Lu, Wang, Peng, Shimoda, & Sylvester, 2009).

In this study, we have examined the preventive and reversal (or therapeutic) effects of TMP in animal models of PH and in patients with PAH. We also examined the cellular and molecular mechanisms involved in the therapeutic effect of TMP, specifically focusing on the signalling pathways associated with Ca^{2+} influx through SOCC and ROCC. Our results suggested that TMP is potentially a safe and effective medication with affordable cost for the treatment of patients with PAH, a disease that is associated with considerable mental and economic burden.

2 | METHODS

2.1 | Animals

All animal care and experimental procedures were approved by the Animal Care and Use Committee of The First Affiliated Hospital of Guangzhou Medical University. Animal studies are reported in compliance with the ARRIVE guidelines (Kilkenny et al., 2010) and with the recommendations made by the *British Journal of Pharmacology*.

Male Sprague-Dawley (SD) rats (RRID: RGD_70508, 150-200 g) and male C57BL/6 mice (RRID:MGI:5653791; 20-25 g) were purchased from Guangdong Provincial Medical Experimental Animal Centre and raised in the Specific Pathogen Free (SPF) grade animal room of the State Key laboratory of Guangzhou Medical University. The animal studies were designed to generate groups of equal size, using randomization and blinded analysis. However, group sizes were sometimes unequal due to the purpose of multiple assays and unexpected loss of individual animals during the procedures.

2.2 | Models of pulmonary hypertension (PH)

Different rat PH models were induced and developed according to previous publications (Shimoda, Sham, & Sylvester, 2000; Wang et al., 2006). Rats were randomly divided into the prevention and treatment models of three commonly used PH models: chronic hypoxia-induced PH (chronic HPH), Sugen/hypoxia-induced PH (SuHx-PH) and monocrotaline (MCT)-induced PH (MCT-PH). These procedures are outlined in Figure 1A (prevention model) and Figure 2A (treatment model). In the chronic HPH group, rats were housed in chronic normobaric hypoxia (10% O_2) for 21 or 35 days. In the SuHx-PH group, each rat was given a single injection of Sugen (SU5416, 20 mg·kg^{-1}; MedChemExpress, USA) on the day before 3 weeks of normobaric hypoxia (10% O_2) followed by 2 weeks of normoxia (21% O_2). In the MCT-PH group, each rat was given a single injection of MCT (50 mg·kg^{-1}, i.p.).

All TMP treatment groups were gavaged daily with TMP (100 mg·kg^{-1}·day^{-1}), while the vehicle control groups were given equivalent volume of saline. In the prevention studies, TMP
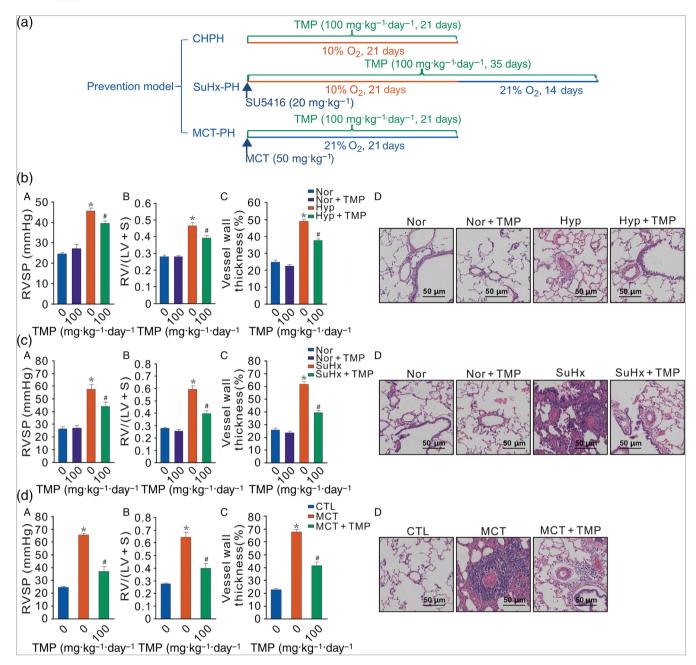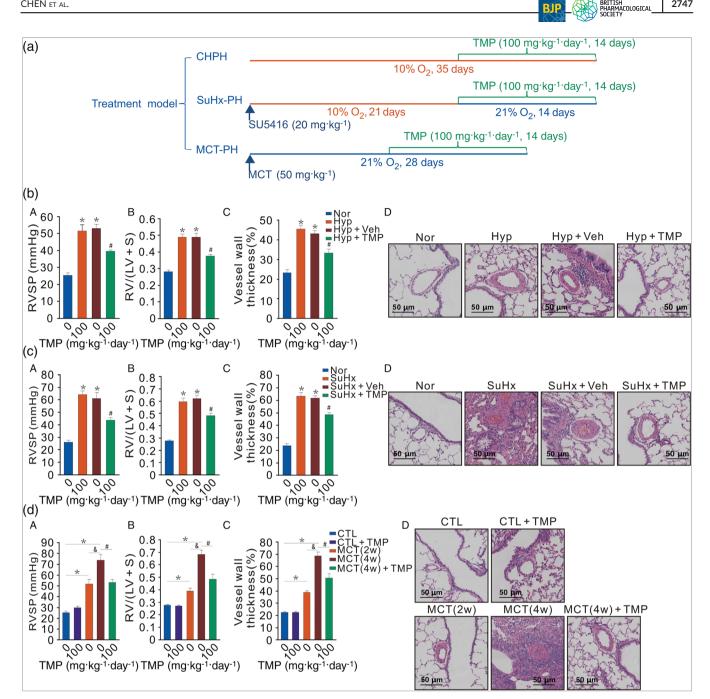
FIGURE 1 TMP attenuates the development of PH in rats with experimental pulmonary hypertension (PH). (a) Diagram showing the protocols for the three prevention rat models of PH: chronic hypoxia-induced PH (CHPH), monocrotaline-induced PH (MCT-PH), and Sugen/hypoxia-induced PH (SuHx-PH). (b) Summarized data (mean ± SEM) showing RVSP (A), Fulton Index (B) and pulmonary arterial wall thickness (C), and representative H&E images (D) of the cross sections of distal PA, in normoxic control rats (Nor) and rats exposed to chronic hypoxia (Hyp) with (TMP, 100 mg·kg^{-1}·day^{-1}) or without (0 mg·kg^{-1}·day^{-1}) treatment of TMP. *$P < .05$, significantly different from Nor group (with 0 mg·kg^{-1}·day^{-1} TMP), #$P < .05$, significantly different from Hyp group. (c) Summarized data (mean ± SEM) showing RVSP (A), Fulton Index (B) and pulmonary arterial wall thickness (C), and representative H&E images (D) of the cross sections of distal PA, in Nor rats and Sugen-injected hypoxic rats (SuHx) with (TMP, 100 mg·kg^{-1}·day^{-1}) or without (0 mg·kg^{-1}·day^{-1}) treatment of TMP. *$P < .05$, significantly different from Nor group (with 0 mg·kg^{-1}·day^{-1} TMP), #$P < .05$, significantly different from SuHx group. (d) Summarized data (mean ± SEM) showing RVSP (A), Fulton Index (B) and pulmonary arterial wall thickness (C), and representative H&E images (D) of the cross sections of distal PA, in control rats (CTL) and MCT-injected rats (MCT) with (TMP, 100 mg·kg^{-1}·day^{-1}) or without (0 mg·kg^{-1}·day^{-1}) treatment of TMP. *$P < .05$, significantly different from CTL group (with 0 mg·kg^{-1}·day^{-1} TMP), #$P < .05$, significantly different from MCT group (with 0 mg·kg^{-1}·day^{-1} TMP). $n = 6$–10 rats in each of the groups

treatment was started on day-1 for a duration of 3 weeks (Nor +TMP, Hyp+TMP and MCT+TMP) or 5 weeks (Nor+TMP and SuHx+TMP). In the treatment studies, TMP treatment was given

daily for 2 weeks starting on day-21 of the 35 days of hypoxic exposure (Hyp+TMP). TMP treatment was started on day-21 when the rats were taken out of hypoxia in the SuHx rat model (SuHx

FIGURE 2 TMP reverses established pulmonary hypertension (PH) in rats. (a) Diagram showing the reversal (treatment) protocols for the three rat models of PH: chronic hypoxia-induced PH (CHPH), monocrotaline-induced PH (MCT-PH), and Sugen/hypoxia-induced PH (SuHx-PH). (b) Summarized data (mean ± SEM) showing RVSP (A), Fulton Index (B) and pulmonary arterial wall thickness (C), and representative H&E images (D) of the cross sections of distal PA, in normoxic control rats (Nor) and rats exposed to chronic hypoxia (Hyp, 5w) with (TMP, 100 mg·kg^{-1}·day^{-1}) or without (0 mg·kg^{-1}·day^{-1}) treatment of TMP or with vehicle treatment (Veh). *$P < .05$ versus Nor group without TMP; #$P < .05$ versus Hyp group with Veh treatment. $n = 6-8$ rats in each group. (c) Summarized data (mean ± SEM) showing RVSP (A), Fulton Index (B) and pulmonary arterial wall thickness (C), and representative H&E images (D) of the cross sections of distal PA, in Nor rats and sugen-injected hypoxic rats (SuHx) with (TMP, 100 mg·kg^{-1}·day^{-1}) or without (0 mg·kg^{-1}·day^{-1}) TMP treatment or with vehicle (Veh) treatment. *$P < .05$ versus Nor group without (0 mg·kg^{-1}·day^{-1}) TMP treatment; #$P < .05$ versus SuHx group with Veh treatment. $n = 6-8$ rats in each group. (d) Summarized data (mean ± SEM) showing RVSP (A), Fulton Index (B) and pulmonary arterial wall thickness (C), and representative H&E images (D) of the cross sections of distal PA, in control rats (CTL) and rats 2 weeks (2w) and 4 weeks (4w) after MCT injection with (TMP, 100 mg·kg^{-1}·day^{-1}) or without (0 mg·kg^{-1}·day^{-1}) treatment with TMP. *$P < .05$, $^{\&}P < .05$, #$P < .05$ versus different groups as indicated with the horizontal bars; $n = 6-8$ rats in each group

+TMP). Treatment of TMP in the MCT rats started on day-14 (MCT+TMP) for a period of 14 days. The vehicle used for MCT is a 2:8 (v/v) mixed solution of ethanol and saline, and for SU5416 is a 4:6 (v/v) mixed solution of DMSO and CMC, which contains 0.5% (w/v) sodium carboxymethyl cellulose, 0.5% (w/v) sodium chloride, 0.4% (v/v) polysorbate 80, 0.9% (v/v) benzyl alcohol diluted in deionized water. All the control animals were vehicle injected. All the groups of rats were blindly labelled when the experiment was terminated. All the rats were killed with an overdose of 3% pentobarbital sodium after haemodynamic measurements.

2.3 | Haemodynamic measurements and lung histology

Procedures were performed as previously described (Lu et al., 2010). Briefly, after the establishment and treatment of the animal models, rats were anesthetized with 3% pentobarbital sodium (30 mg· kg^{-1}, i. p.). Right ventricular pressure was measured using a 23-gauge needle filled with 0.3% heparinized saline connected to a pressure transducer and a BIOPAC MP150 data acquisition system (BIOPAC systems, Inc., Santa Barbara, CA). The fluid-filled needle was inserted into the right ventricle (RV) via the diaphragm. Right ventricular hypertrophy was evaluated by: a) the ratio of RV weight to left ventricle (LV)+ septum (S) weight [RV/(LV+S)], and b) the ratio of RV weight to the body weight. The lungs from control and PH-model rats were prepared by flushing the right ventricle with 5 ml of saline, until the aortic outflow was clear. The lungs were fixed under 20 cm H$_2$O constant pressure by 4% paraformaldehyde, embedded in paraffin and sectioned at 5 μm thickness. Sections were stained with haematoxylin and eosin (H&E staining).

2.4 | Measurements in isolated perfused lung

These experiments were carried out with male C57BL/6 mice, using the isolated, perfused and ventilated ng preparation described by Yoo et al. (2013). Briefly, mice were deeply anesthetized with ketamine (100 mg·kg^{-1}) and xylazine (26 mg·kg^{-1}) via an intra-abdominal injection and ventilated with a gas mixture of 21% O$_2$, 5% CO$_2$ via a rodent ventilator (Minivent type 845, Harvard Apparatus, USA). Respiratory rate was maintained at 80 breaths min^{-1} and tidal volume was 10 ml·kg^{-1} (~250 ml). Positive end-expiratory pressure was maintained at 2 mm H$_2$O. End-inspiratory plateau pressure (EIP) was measured by a pressure transducer (MPX type 399/2, Hugo Sachs Elektronik-Harvard Apparatus, Germany) which was connected to a tracheal catheter. The mice were secured in the chamber of the isolated perfused lung system (IL-1 Type 839, Harvard Apparatus, USA), the chest was opened by median sternotomy, and then the pericardium, thymus, and fat tissue were carefully removed. In order to prevent blood coagulation, 20 IU heparin was injected into the right ventricle. A stainless steel catheter was inserted into the main pulmonary artery

(PA) after performing a right ventriculotomy, and the PA and ascending aorta were tied together using a 6-0 black silk suture. Pulmonary arterial pressure (PAP) was measured using a pressure sensor (P75 Type 379, Hugo Sachs Elektronik-Harvard Apparatus, Germany), which was connected to the PA catheter. The other end of the catheter was connected to a tube for pulmonary perfusion. After a small incision of the left ventricle, the mitral valve was opened using a small haemostat, and the stainless steel cannula was inserted into the left atrium via a left ventriculotomy, which was drained into the reservoir. This cannula was fixed by a black silk suture, which was tied to the left ventricular wall. The pulmonary circulation was maintained in a closed circuit via a peristaltic pump (ISM 834, ISOMATEC, USA). The total volume of perfusate was 50 ml and the flow rate was maintained at 2 ml·min^{-1}. The PAP, left atrial pressure, and EIP were monitored continuously. Before each cannula was inserted, the pressure was zeroed at the height of the heart. For data acquisition and data storage, Powerlab 8/30, Quad Bridge Amp, and LabChart (AD Instruments, Australia) were used. To maintain the humidity of the opened lung, physiological saline was applied to the thoracic cavity. Temperature was maintained at 36-38°C with a water jacket in the chamber and reservoir. Once the basal PAP had been stabilized for 40-60 minutes, the experiments were performed.

2.5 | Isometric tension measurement using rings of intralobar PAs

Rats were killed, and the heart and lung were quickly removed from each animal and placed in Krebs-Henseleit solution. The tertiary-branch PAs (external diameter <0.35 mm) were separated carefully and were cut into 3-mm-length rings. Separated PA rings were suspended in parallel by two stainless-steel wires in an organ bath. One stirrup was connected to an isometric force transducer to measure tension of the vessels. The rings were stretched until they exerted an optimal basal tension of 0.8 g, and then were allowed to equilibrate for 100 minutes with the bath solution replaced every 20 minutes. The solution was bubbled with 95% O$_2$+5% CO$_2$. Isometric tension of isolated PA rings precontracted by phenylephrine (1 μM), and the effects of TMP were determined in the presence or absence of endothelium. After isolation of the PA ring, the endothelium was removed by inserting a stainless steel wire and gently twisted to disrupt the endothelium without affecting the smooth muscle layer. The PA rings were exposed to KCl (60 mM) three times to establish viability and maximum contraction and to phenylephrine (1 μM) followed by ACh (10 μM), known to induce endothelium-dependent vasodilation, to confirm the presence or absence of endothelium. In endothelium-denuded PAs, phenylephrine (1 μM) induced no significant contraction in calcium free solution, while restoration of calcium in the perfusate can induce significant vasocontraction mediated by phenylephrine. Therefore, the effects of pretreatment with and without TMP (160 μM) of CaCl$_2$ (0-2.5 mM)-mediated maximal contraction in response to phenylephrine

(1 μM) were also recorded and analyzed. Moreover, to further elucidate the potential roles of K^+ channels in TMP-mediated acute vasodilatation, we then introduced a 30-min pretreatment with specific inhibitors to block the four K^+ channels: the K_{IR} inhibitor, $BaCl_2$ (100 μM); the K_{ATP} channel inhibitor, **glibenclamide** (10 μM); the K_V channel inhibitor **4-AP** (1 mM) and the K_{Ca} inhibitor **TEA** (10 mM). The effects of these specific K^+ channels in TMP-mediated vasodilation were also tested in endothelium-denuded PA rings.

2.6 | Isolation and culture of primary rat distal PASMCs

The rat distal PASMCs were identified and cultured as previously described (Wang, Shimoda, & Sylvester, 2004). Distal (>4th generation) intrapulmonary arteries were dissected from the lungs of different groups of rats in both the prevention and treatment models. Adventitia was removed, and endothelium was denuded by opening the vessel longitudinally and rubbing the luminal surface with a cotton swab carefully. The PASMCs were enzymically dissociated from these tissues, seeded in culture dishes and cultured for 3-4 days in SMGM-2 culture media containing 5% FBS in a humidified atmosphere of 5% CO_2-95% air at 37°C. Cell purity was assessed by the morphological features under a phase-contrast microscopy and immunofluorescence staining for specific smooth muscle cell markers α-actin and myosin heavy chain under fluorescent microscopy.

For prolonged hypoxia and TMP treatment, after cells had grown to 60-70% confluence, the culture media was replaced with SMBM basal culture media supplemented with 0.3% FBS for 24 hours to allow cells for growth arrest, and then exposed to prolonged hypoxia (4% O_2) or normoxia in the presence or absence of TMP (6.25 μM). The O_2 concentration in the culture incubator was continuously monitored and modulated in real time with an O_2 sensor and a switch controlling nitrogen gassing. The cells isolated from distal PAs of chronic HPH rats were transiently seeded in Ham's F-12 medium with L-glutamine (Jinuo Co. Ltd, Hangzhou) supplemented with 0.5% FBS for 24 hours before [Ca^{2+}]i measurement.

2.7 | Cell proliferation assay

The cell proliferation was assessed by an Amersham Cell Proliferation Biotrak ELISA kit (GE health care, Buckinghamshire, UK). Cells were seeded into 96-well plates at 4×10^3 cells per well and cultured for 24 hours in SMGM-2 complete medium. After a further 24-hour culture in SMBM containing 0.3% FBS, the cells were subjected to TMP (0-200 μM) treatment for 60 hours with or without hypoxic (4% O_2) exposure. The labelling reagent containing 5'-bromo-2'-deoxyuridine (BrdU) was added to the cells and incubated for 24 hr and subsequent ELISA assay for BrdU incorporation was performed according to the manufacturer's instruction.

2.8 | Cytotoxicity assessment

The cytotoxic effect of TMP on PASMCs was analyzed using the CytoTox-Glo Cytotoxicity Assay kit (Promega, Madison, WI) according to the manufacturer's instruction. The assay sensitivity was determined by running a series of two-fold dilutions of cells from 1×10^4 per well to 1.56×10^2 per well in a 96-well culture plate, and the signal to noise (S:N) was calculated. Based on the determined assay sensitivity, PASMCs were plated at 5×10^3 cells per well in 96-well plates, incubated for 60 hr, with or without TMP (0-25 μM) under normoxia or hypoxia, and subjected to cytotoxicity measurements. Cell viability was calculated as percentage ratios of luminescence for viable cells to total per treatment well.

2.9 | Cell migration experiment

PASMCs treated with TMP (0-25 μM) for 60 hr under normoxic or hypoxic conditions were trypsinized and loaded on the 8 μm polycarbonate membrane of Transwell Permeable Support (24 mm, Corning Inc., Corning, NY) (2×10^3 cells per well) equilibrated with SMBM containing 0.3% FBS. After 24-hour culture, cells were fixed with 95% freezing-cold ethanol, followed by staining with Brilliant Blue R Staining Solution (Sigma) which contained 0.5% (w/v).

Brilliant Blue R, 45% ethanol and 10% acetic acid for 5 minutes and washing with PBS. The stained cells were observed under an inverted microscope. Five photographs were taken at fixed positions of the Transwell membrane: top left and right, bottom left and right and the central area. The cells on these photos were counted as total cells. Cells on the upper surface of the membrane were then gently wiped off with a cotton swab. In the same fields as indicated above, photos of the lower surface of the membrane were taken. Cells on the lower surface of the membrane are the migrated cells. The migration rate is the ratio of migrated cells to the total cells.

2.10 | Intracellular calcium concentration, [Ca^{2+}]$_i$, measurements

[Ca^{2+}]$_i$ and increase in [Ca^{2+}]$_i$ due to SOCE were measured with Fura-2-AM dye (Molecular Probes, Eugene, OR) and fluorescent microscopy as previously described (Lu et al., 2010; Wang et al., 2004; Wang et al., 2006). Coverslips with PASMCs were incubated with 5 μM Fura-2-AM for 60 minutes at 37°C in 5% CO_2-95% air. The coverslips were mounted in a closed polycarbonate chamber and clamped in a heated aluminum platform (PH-2, Warner Instrument Corporation, Hamden, CT) on the stage of a Nikon TSE 100 Ellipse inverted microscope (Nikon, Melville, NY). The chamber was perfused at 0.5 ml min^{-1} with Krebs Ringer bicarbonate solution (KRBS). The KRBS, containing (in mM) 118 NaCl, 4.7 KCl, 0.57 $MgSO_4$, 2.5 $CaCl_2$, 25 $NaHCO_3$, 1.18 KH_2PO_4, and 10 glucose, was equilibrated with 16% O_2-5% CO_2 at 38°C in heated reservoirs and passed via stainless steel tubing and a manifold to an in-line heat exchanger (SF-28,

Warner Instrument Corporation, Hamden, CT) before it entered the cell chamber. The temperature of the chamber and the heat exchanger was controlled by a dual channel heater (TC-344B, Warner Instrument Corporation, Hamden, CT). This system maintained the temperature at 37°C and oxygen tension at 112±2.0 mmHg at the cover slip. After perfusing for 10 minutes to remove extracellular dye, ratiometric measurement of Fura-2 fluorescence was performed at 12-30 seconds intervals with a collimated light beam from a xenon arc lamp fitted with interference filters at 340 and 380 nm and focused onto PASMCs visualized with a 20× fluorescence objective (Super Fluor 20, Nikon, Torrance, CA). Light emitted from the cells at 510 nm was returned through the objective and detected by a cooled CCD imaging camera. An electronic shutter (Vincent Associates, Rochester, NY) was used to minimize photobleaching. Data were collected on-line with InCyte software (Intracellular Imaging Inc, Cincinnati, OH). The $[Ca^{2+}]i$ was reflected by the ratio of $F340/F380$ created by measuring Fura-2 fluorescence. To assess SOCE, PASMCs were perfused for at least 10 minutes with Ca^{2+}-free KRBS containing 5 μM of nifedipine to inhibit Ca^{2+} entry through L-type voltage-dependent Ca^{2+} channels (VDCC) and 10 μM of CPA to deplete SR Ca^{2+} stores. Next, we examined Fura-2 fluorescence excited at 360 nm at 30 seconds intervals before and after addition of $MnCl_2$ (200 μM) to the perfusate, and SOCE was evaluated from the rate at which Fura-2 fluorescence was quenched by Mn^{2+}, which entered the cells as Ca^{2+} surrogates and reduced Fura-2 fluorescence upon binding to the dye. Fluorescence excited at 360 nm is the same for both Ca^{2+}-bound and Ca^{2+}-free Fura-2; therefore, changes of fluorescence can be assumed to be caused by Mn^{2+} alone. In the experiment evaluating the effect of membrane potential change on Mn^{2+} quenching, NaCl was replaced with equimolar KCl in the perfusate with final concentration of KCl at 122.7 mM. To obtain statistically significant results, the fluorescence intensity was determined in at least 20 cells for each sample.

2.11 | Real-time quantitative PCR (RT-qPCR)

The total RNA from the PAs and the PASMCs was extracted with the TRIZOL (Invitrogen, Carlsbad, CA) method as previously described (Lu, Wang, Shimoda, & Sylvester, 2008; Wang et al., 2004; Wang et al., 2006). DNA contamination in the RNA preparation was removed by on-column DNase digestion with RNeasy column and RNase-free DNase (Qiagen). Reverse transcription was performed with Takara RT kit (Takara, Dalian, China) with reaction system containing 1 μg total RNA in a 20 μl volume. cDNA of rat TRPC1, TRPC6 or 18s were amplified by real-time quantitative PCR (RT-qPCR) with Scofast TM EvaGreen SuperMix (Bio-Rad, Carlsbad, CA) in a CFX96 TM real-time system (Bio-Rad). The PCR protocol consisted of initial enzyme activation at 95°C for 3min, followed by 40 cycles at 95°C for 5s and at 60°C for 15s.

Primer sequences were as follows: TRPC1: sense, 5'-AGCCTCTT GACAAACGAGGA-3', anti-sense,5'-ACCTGACATCTGTCCGAACC-3'; TRPC6: sense, 5'-TACTGGTGTGCTCCTTGCAG-3', anti-sense, 5'-

GAGCTTGGTGCCTTCAAATC-3'; 18s: sense, 5'-GCAATTATTCCCCA TGAACG-3', anti-sense, 5'-GGCCTCACTAAACCATCCAA-3'. Relative concentration of each transcript was calculated with the Pfaffl (2001) method. Efficiency for each gene was determined from 5-point serial dilutions of an unknown cDNA sample (PAs or PASMCs). The expression of TRPC1 and TRPC6 were normalized to that of 18s as a housekeeping gene.

2.12 | Western blotting

The immuno-related procedures used comply with the recommendations made by the British Journal of Pharmacology (Alexander et al., 2018). The procedure for isolation of total protein was performed, probed, and measured by immunoblotting as described (Lin et al., 2004; Lu et al., 2010; Wang et al., 2006). Both the PAs and PASMCs were sonicated and lysed in TPER lysis buffer (Pierce, Rockford, IL) supplemented with protease inhibitor cocktail, and TRPC expression was measured by immunoblotting assay. The nuclear and cytoplasm protein fractions isolation was performed following the protocols provided with the kit (Thermo Scientific Inc.), and then measured by Western blot. The specific primary antibodies and concentration we used were: TRPC1 (Abcam, 1:1000 dilution), TRPC6 (Abcam, 1:1000 dilution), HIF-1α (Abcam, 1:500 dilution) and smooth muscle α-actin (Sigma, 1: 10000 dilution).

2.13 | Echocardiographic measurements

The rats from the different experimental groups were maintained under anesthesia, with spontaneous breathing, by 5% isoflurane. Then, the dose of anesthetics was reduced to 2% and the echocardiographic measurements were performed. During the echocardiographic examination, the body temperature of rats was maintained by a heating plate. Transthoracic 2-dimensional (2D), Pulsed-Wave Doppler Mode and M-mode imaging were performed with the Vevo 2100 Imaging System (Visual Sonics, Toronto, Canada) with a 13-24 MHz transducer (MS250, Visual Sonics, Toronto, Canada). The images were stored on a computer for subsequent analysis. Each parameter was measured and averaged over 3 cardiac cycles. The pulmonary arterial acceleration time (PAT) was used as an echocardiographic indicator of pulmonary hypertension was measured from pulmonary artery near pulmonary valves. It was normalized to pulmonary arterial ejection time (PET) as measured within the same images. Right ventricular end diastolic diameter (RVEDD) and right ventricular end-diastolic free-wall thickness (RVEDWT) were used to assess the RV morphology. Both of these indices were measured in the long-axis parasternal view by M-mode. Fractional area change (FAC) and tricuspid annular plane systolic excursion (TAPSE) were used to assess RV function. FAC was measured under 2D echocardiographic guidance from the apical 4-chamber view. TAPSE was measured under 2D echocardiographic guidance or by Mmode from the apical 4-chamber view.

2.14 | Randomized controlled clinical trial

The randomized controlled trial was conducted at the First Affiliated Hospital of Guangzhou Medical University, and was approved by the ethics committee of Guangzhou Medical University (www.chictr.org.cn number: ChiCTR-IPR-14005379). A total of 12 comparator and 24 TMP-treated patients were involved. All patients gave informed consent under the guidelines of the ethics committee of the First Affiliated Hospital of Guangzhou Medical University.

Subjects were included in the study if they had a mean pulmonary arterial pressure (mPAP) of greater than or equal to 25 mmHg at rest as assessed by right heart catheterization (RHC), diagnosed with either Pulmonary arterial hypertension (PAH) or chronic thromboembolic pulmonary hypertension (CTEPH) and had a WHO PH functional class of II, III or IV. Patients with other forms of PH were excluded (PH in the setting of left heart disease, PH in the setting of lung disease or PH with unclear multifactorial mechanisms). Patients were also excluded if they had no legal capacity, were pregnant or nursing; had a significant history of immunosuppressive or allergic disorder; a creatinine clearance (Ccr) $\leq$ 50 ml·min^{-1}; an abnormal liver function tests (i.e., alanine transferase >80 IU·L^{-1} and aspartate transferase >42 IU·L^{-1}), and were positive for hepatitis B surface antigen or HIV.

For all the recruited subjects, background therapy was given for the treatment of pulmonary hypertension (including phosphodiesterase 5 inhibitors, soluble guanylate cyclase agonists, endothelin receptor antagonists, prostacyclin and its analogues/receptor agonists). Then, at the time of initial enrollment, subjects were randomized at a 2:1 ratio (TMP:Comparator) to receive study medication (100 mg, t.i.d.) or equal amount of placebo. All patients received standard clinical therapy for pulmonary hypertension including cardiac, diuretic, anticoagulation and targeted drugs for 16 weeks. During the study, patients came in every 4 weeks for a 6-minute walk test. At baseline, 8 weeks and 16 weeks, patients also underwent an echocardiogram, a CT examination, and standard blood work per standard clinical routine. RV systolic pressure, left ventricular ejection fraction (LVEF) and right atrial diameter were measured.

2.15 | Data and statistical analysis

The data and statistical analysis comply with the recommendations of the *British Journal of Pharmacology* on experimental design and analysis in pharmacology (Curtis et al., 2018). Continuous variables were expressed as mean ± SEM or mean ± SD as indicated. Satistical analysis was undertaken only for studies where each group size was at least n = 5. All the declared group size is the number of independent values and that statistical analysis was done using these independent values, not technical replicates. The study data were analysed statistically with two-way repeated measure ANOVA (general linear model) and Friedman's two-way repeated ANOVA test. As for two-way repeated measure ANOVA, the study explored differences of the two groups by tests of between-subject effects. When assumption of sphericity was violated, the result was corrected by Greenhouse–Geisser. The

difference between the two groups and interaction between the time courses and groups were obtained. In multigroup studies with parametric variables, post hoc tests were conducted only if F in ANOVA (or equivalent) achieved the necessary level of statistical significance, and there was no significant variance inhomogeneity. Bonferroni post hoc tests were conducted only if differences in two groups were statistically significant, and there was no variance inhomogeneity. In Friedman's two-way repeated ANOVA test, a non-parametric test was used if the variable was not normally distributed. The categorical variables - pericardial effusion, and WHO PH functional class - were analysed by generalized estimating equations. Differences were considered to be significant when P <.05. All the data including the outliers were included in data analysis and presentation. We ensure that all the calculation of the data and the data units fits with the Y axis that is labelled in the figures.

2.16 | Materials

The TMP used for the in vitro experiments was purchased from the Chinese National Institute for Food and Drug Control (Beijing, China), in the form of TMP phosphate monohydrate ($C_8H_{12}N_2 \cdot H_3PO_4 \cdot H_2O$; MW 252.20 g·mol^{-1}) and from Sigma-Aldrich Corp. Inc. ($C_8H_{12}N_2$; MW 136.19 g·mol^{-1}, St. Louis, MO, USA). For the animal experiments and the clinical trial, TMP pills were purchased from Livzon Pharmaceutical Group Inc. (National Approval Certificate Number H4424348). Each pill contains 50 mg TMP. A dose of 100 mg·kg^{-1}·day^{-1} (administered by gavage) was used for the in vivo animal experiments, and a dose of 100 mg of TMP (t.i.d) was used in the clinical trial. Glibenclamide, 4-AP, TEA and phenylephrine were supplied by Sigma-Aldrich Corp. Inc (Table 5).

2.17 | Nomenclature of targets and ligands

Key protein targets and ligands in this article are hyperlinked to corresponding entries in http://www.guidetopharmacology.org, the common portal for data from the IUPHAR/BPS Guide to PHARMACOLOGY (Harding et al., 2018), and are permanently archived in the Concise Guide to PHARMACOLOGY 2019/20 (Alexander, Fabbro et al., 2019; Alexander, Mathie et al., 2019).

3 | RESULTS

3.1 | TMP attenuates the development and progression of experimental PH in rats

To examine the therapeutic effects of TMP, we first conducted the prevention experiments using three different animal rat models of PH: (a) chronic hypoxia-induced PH (chronic HPH), (b) hypoxia- and Sugen-induced PH (SuHx-PH), and (c) MCT-induced PH (MCT-PH). Rats exposed to sustained normobaric hypoxia (10% O_2 for 21 days) developed significant PH, determined by increased right ventricular systolic pressure (RVSP) in hypoxic rats, compared with those in

normoxic rats (Figure 1b – A). Rats exposed to hypoxia also exhibited RV hypertrophy reflected by increased ratio of [RV/(LV+S)] (Fulton Index, Figure 1b – B) and pulmonary vascular remodelling with thickening of distal PA wall (Figure 1b – C and D). Initiation of TMP treatment (100 mg·kg^{-1}·day^{-1}, gavage) significantly attenuated the hypoxia-induced increases in RVSP (Figure 1b – A), attenuated the Fulton Index (Figure 1b – B) and vascular remodelling (Figure 1b – C and D). These data indicated that daily treatment of TMP is effective in inhibiting the development of chronic HPH. In parallel, SuHx-PH and MCT-induced PH rats also developed significant PH. Daily treatment with TMP starting on Day 0 significantly attenuated the development and progression of experimental PH in both the SuHx-PH (Figure 1c) and MCT-PH models (Figure 1d).

3.2 | TMP reverses established PH in rats with HPH, SuHx-PH, and MCT-PH

We then evaluated the potential of TMP for reversal of established PH in rats with hypoxia-induced PH, hypoxia/Sugen-induced PH, and MCT-induced PH. As shown in Figure 2, by 3 weeks in the chronic HPH and SuHx-PH models, as well as 2 and 4 weeks in the MCT-PH model, there was already a manifestation of PH, as measured by increased RVSP in the HPH (Figure 2b – A) and in the SuHx-PH (Figure 2c – A) rats, as well as in the MCT-PH rats, after 2 weeks and 4 weeks (Figure 2d – A).

In the HPH model, 2 weeks of TMP treatment starting 3 weeks after chronic HPH decreased RVSP, associated with a decrease in pulmonary vascular remodelling and RV hypertrophy. In the SuHx-PH model, 2 weeks of TMP treatment decreased RVSP (Figure 2c – A). In the more severe MCT-PH model, RVSP increased as early as 2 weeks of MCT treatment (Figure 2d – A), while 2 weeks of TMP treatment lowered the RVSP in the MCT group. Moreover, in all three rat models of established PH, a 2-week treatment of TMP also markedly reversed the RV hypertrophy, determined by the Fulton Index or the ratio of RV weight to the sum of LV and septum (S) weight [RV/(LV+S)] (Figure 2b,c,d – B), and the vascular remodelling (Figure 2b,c,d – C and D) without affecting the control rats.

3.3 | TMP sufficiently improves the right heart function in all the three PH models of both prevention and treatment models

We also performed echocardiographic analysis to determine the effects of TMP on the cardiac function. As shown in Figure 3, all three PH models exhibited significant impairment of the right heart function, determined by fractional area change (FAC), tricuspid annular plane systolic excursion (TAPSE), RV end-diastolic free-wall thickness (RVEDWT), RV end-diastolic diameter (RVEDD), and pulmonary acceleration time/pulmonary ejection time (PAT/PET). As shown in Figure 3, TMP treatment reversed the right heart dysfunction. Left ventricular function was not significantly changed in all three PH models, and TMP treatment had no effect on the left heart function

parameters: left ventricular ejection fractions (LVEF) and left ventricular fractional shortening (LVFS; Figure S2).

3.4 | TMP inhibits hypoxia-induced increase in PAP in isolated perfused/ventilated mouse lung

To examine the effect of TMP on acute hypoxia-induced pulmonary vasoconstriction or increase in PAP, we used an isolated perfused/ventilated mouse lung system (Yoo et al., 2013). As shown in Figure 4a, acute alveolar hypoxia rapidly increased the mPAP from baseline by causing pulmonary vasoconstriction. Acute treatment with TMP (2.5 mM for 10 min) not only decreased the resting PAP under normoxic conditions (Figure 4a – B) but also significantly inhibited hypoxia-induced increase in PAP (Figure 4a – C). These data indicate that TMP has an acute vasodilatory effect on the pulmonary vasculature and can efficiently inhibit alveolar hypoxia-induced pulmonary vasoconstriction.

3.5 | TMP dose-dependently reduces contraction induced by phenylephrine in PA rings in an endothelium-independent manner

To further examine the effect of TMP on pulmonary vasoconstriction and vasodilation, we measured the isometric tension in rings of isolated intralobar pulmonary arteries (PAs). We found that TMP dose-dependently decreased the contraction of PA rings induced by 1 μM phenylephrine (Figure 4b). The TMP-induced relaxation was independent of endothelium, as the dose-dependent relaxant effect of TMP in the endothelium-intact PA rings was the same as the effect in the endothelium-denuded PA rings (Figure 4b – A). Furthermore, pretreatment of the endothelium-denuded PA with 160 μM TMP significantly inhibited the Ca^{2+}-dependent pulmonary vasoconstriction in PA rings constricted with 1 μM phenylephrine (Figure 4b – B), as the maximal tension induced by 2.5 mM Ca^{2+} in the presence of phenylephrine was decreased by TMP (Figure 4b – B).

To further elucidate the potential roles of K$^+$ channels in the acute vasodilator effect mediated by TMP, we then used specific inhibitors to block the four K$^+$ channels: Ba^{2+} for blocking K$_{IR}$ channels, glibenclamide for blocking K$_{ATP}$ channels, 4-AP for blocking K$_V$ channels, and TEA for blocking K$_{Ca}$ channels. As shown in Figure 4c, a 30 min pre-incubation of isolated distal PA rings with the K$_{Ca}$ blocker TEA (10 mM; Figure 4c – A) significantly inhibited the vasodilator effect of TMP, whereas blockers of K$_{IR}$ (BaCl$_2$, 100 μM), K$_{ATP}$ (glibenclamide, 10 μM), and K$_V$ channels (4-AP, 1 mM) channels had no effects on TMP-mediated pulmonary vasodilation (Figure 4c – B–D). These results suggest that the vasodilator effect of TMP is mediated in part by the activation of K$_{Ca}$ channels, which induces K$^+$ efflux and membrane hyperpolarization and repolarization, and subsequently closure of the voltage-dependent Ca^{2+} channels, causing vasodilation.
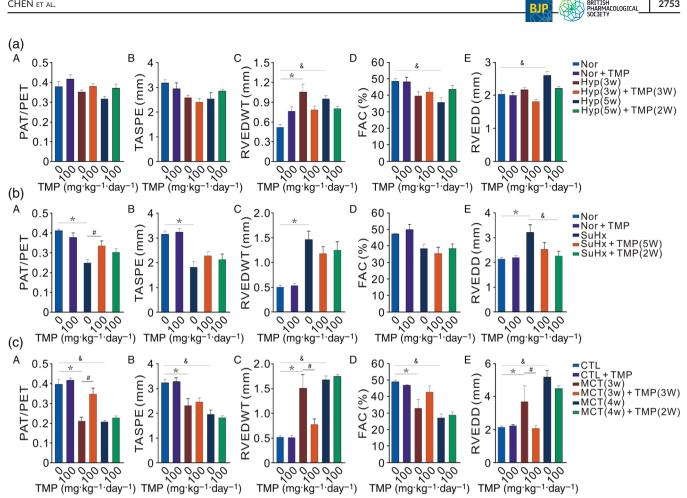
FIGURE 3 Effect of TMP on the right heart function by echocardiographic analysis. (a) Summarized data (mean ± SEM) showing pulmonary acceleration time/pulmonary ejection time (PAT/PET, *A*), tricuspid annular plane systolic excursion (TAPSE, *B*), RV end-diastolic free-wall thickness (RVEDWT, *C*), fractional area change (FAC, *D*), and RV end-diastolic diameter (RVEDD, *E*) in normoxic control rats (Nor) and rats exposed to chronic hypoxia (Hyp) for 3 weeks (3w) or 5 weeks (5w) in the presence (TMP, 100 mg·kg^{-1}·day^{-1} for 3w or 2w) or absence (0 mg·kg^{-1}·day^{-1}) of TMP treatment. *$P < .05$, &$P < .05$, significantly different as indicated. n = 5–11 rats in each group. (b) Summarized data (mean ± SEM) showing PAT/PET (*A*), TAPSE (*B*), RVEDWT (*C*), FAC (*D*), and RVEDD (*E*) in Nor rats and sugen-injected hypoxic rats (SuHx) in the presence (TMP, 100 mg·kg^{-1}·day^{-1} for 3w or 2w) or absence (0 mg·kg^{-1}·day^{-1}) of TMP treatment. *$P < .05$, &$P < .05$, significantly different as indicated. n = 5–11 rats in each group. (c) Summarized data (mean ± SEM) showing PAT/PET (*A*), TAPSE (*B*), RVEDWT (*C*), FAC (*D*), and RVEDD (*E*) in control rats (CTL) and rats 3 weeks (3w) and 4 weeks (4w) after MCT injection in the presence (TMP, 100 mg·kg^{-1}·day^{-1}) of TMP treatment for 3 weeks (3w) or 2 weeks (2w) or absence (0 mg·kg^{-1}·day^{-1}) of TMP treatment. *$P < .05$, &$P < .05$, #$P < .05$, significantly different as indicated. n = 5–11 rats in each group

3.6 | TMP decreases the hypoxia-induced elevation of basal [Ca^{2+}]$_i$ and SOCE in PASMCs

Firstly, we determined the effect of TMP on [Ca^{2+}] and SOCE in cultured rat PASMCs exposed to either normoxia or hypoxia (4% O$_2$, 60 h). In PASMCs exposed to prolonged hypoxia (4% O$_2$, 60 h), the basal [Ca^{2+}]$_i$ was increased, relative to that in cells exposed to normoxia (Fig. 5A). Treatment with TMP (6.25 μM) significantly decreased the basal [Ca^{2+}]$_i$ under hypoxic conditions. Similarly, TMP treatment (6.25 μM) attenuated the hypoxia-induced increase in SOCE (Fig. 5B). Treatment with TMP did not affect the basal [Ca^{2+}]$_i$ or SOCE in PASMCs under normoxia.

Then, to examine the effects of TMP treatment on chronic hypoxia-induced increases in the basal [Ca^{2+}]$_i$ and the enhancement of SOCE, PASMCs were freshly isolated from chronic HPH rats with/without TMP treatment. As shown in Figure 5C, the basal [Ca^{2+}]$_i$ in PASMCs was higher in the cells taken from the chronic HPH group than in those from the normoxia group. The SOCE, determined by Mn^{2+}-mediated fluorescence quenching, was also enhanced in cells taken from the chronic HPH group, compared with that in the normoxic group (Figure 5D). TMP treatment (100 100 mg·kg^{-1}·day^{-1}) decreased the basal [Ca^{2+}]$_i$ and inhibited SOCE in the PASMCs from the chronic HPH group.
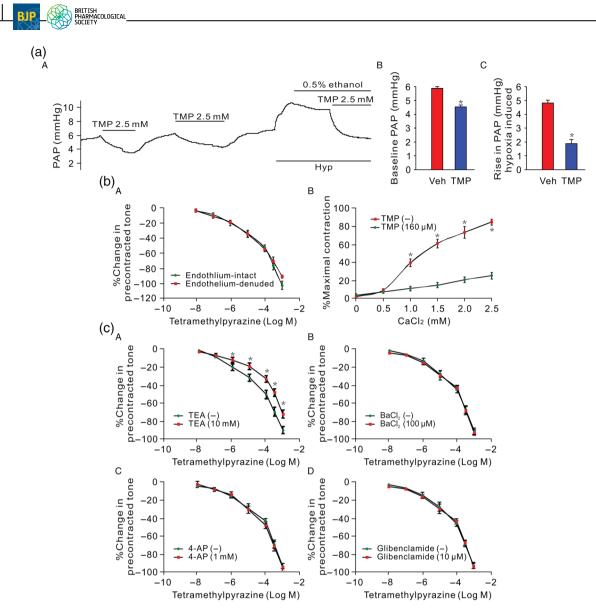
FIGURE 4 Acute vasodilator effect of TMP in isolated perfused/ventilated lung and isolated pulmonary artery. (a) Representative record (A) showing pulmonary arterial pressure (PAP) before, during and after superfusion of TMP (2.5 mM) and before and during alveolar ventilation of hypoxic gas (3% O_2 in N_2) in isolated perfused/ventilated lung. Summarized data (mean ± SE, $n = 8$) showing the hypoxia-induced increase in PAP in the presence of vehicle (Veh, 0.5% ethanol) or TMP (2.5 mM) treatment. *$P < .05$, significantly different from Veh. (b) Dose–response curves (mean ± SEM) of TMP-mediated vasodilation in isolated pulmonary artery rings precontracted with phenylephrine (PE). Panel A, in endothelium-intact or endothelium-denuded PA rings; Panel B, in PA rings superfused with solutions in the presence of increasing concentrations of $CaCl_2$ (from 0 to 2.5 mM), and treated with [TMP (+)] or without [TMP (−)] 160 μM of TMP. *$P < .05$ versus TMP curve. (c) Dose–response curves (mean ± SEM) of TMP-mediated vasodilation in isolated endothelium-denuded pulmonary artery rings precontracted with PE. Panels A–D, in endothelium-denuded PA rings treated with (+) or without (−) 10 mM of TEA (A), with (+) or without (−) 100 μM of Ba^{2+} (B), with (+) or without (−) 1 mM of 4-AP (C), and with (+) or without (−) 10 μM of glibenclamide (D). *$P < .05$, significantly different from TEA (−) curve; $n = 5$ rats for each group

3.7 | TMP inhibits the up-regulation of TRPC1 and TRPC6 in the endothelium-denuded PAs isolated from rats with experimental PH

As shown in Figure 6a–c, the mRNA and protein expression levels of TRPC1 and TRPC6 in the endothelium-denuded rings of PAs isolated from chronic HPH rats were significantly higher than in rings isolated from normoxic controls, while TMP treatment (100 mg·kg^{-1}·day^{-1}) markedly inhibited the hypoxic up-regulation of TRPC1 and TRPC6 at both mRNA and protein levels. Similarly, the protein levels of TRPC1 and TRPC6 were also increased in PA isolated from SuHx-PH rats (Figure 6d) and MCT-PH rats (Figure 6e); and treatment of the SuHX-PH rats and MCT-PH rats with TMP significantly decreased the protein levels of TRPC1/C6 to levels similar to those in normoxic control rats.
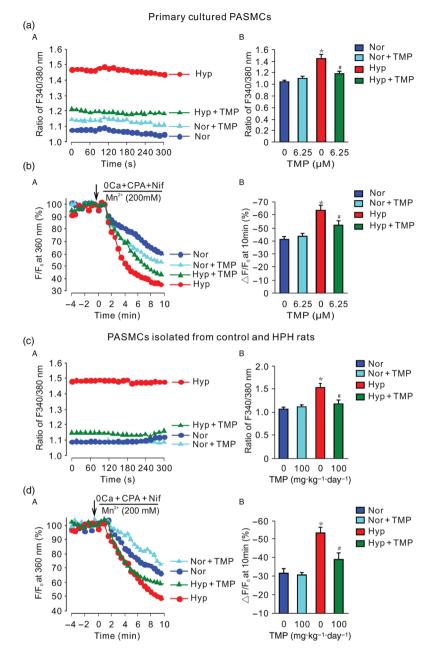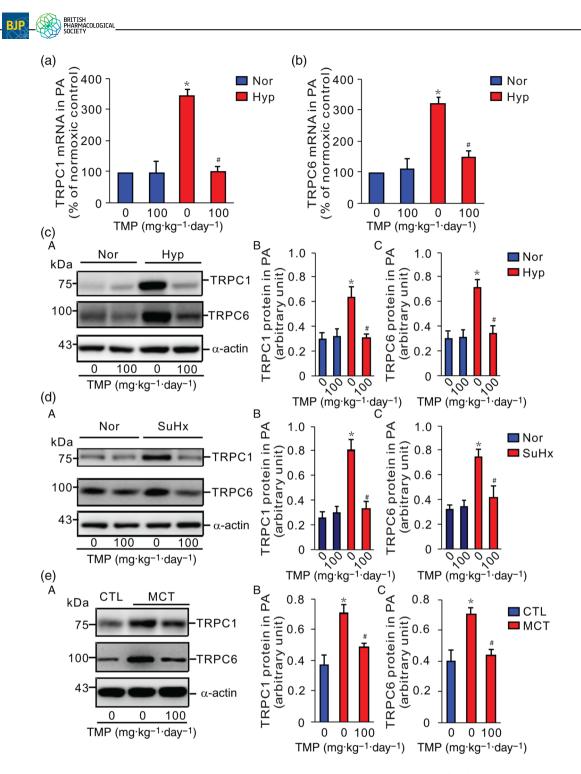
FIGURE 5 TMP inhibits hypoxia-induced increases in the basal $[Ca^{2+}]_i$ and SOCE in PASMCs. (a) Representative records (A) and summarized data (mean ± SEM, B) showing the basal $[Ca^{2+}]_i$, shown as ratiometric fluorescence intensity (F340/380 nm), in PASMCs incubated under normoxic (Nor) and hypoxic (Hyp, 4% O_2 for 60 hr) conditions with (+TMP) or without TMP treatment. Nor, n = 151 cells; Nor + TMP, n = 173 cells; Hyp, n = 185 cells; and Hyp + TMP, n = 154 cells (n = 5 rats for each group). *P < .05, significantly different from Nor (without TMP treatment); #P < .05, significantly different from Hyp (without TMP treatment). (b) Representative records (A) showing Fura-2 fluorescence quenched by 200-mM $MnCl_2$ in cultured PASMCS exposed to normoxia (Nor) or hypoxia (Hyp, 4% O_2 for 6 hr) in the presence (+TMP) or absence of TMP. Data at each time point are normalized to fluorescence at 0 min (F_0) and indicated as the ratio of F/F_0. SOCE is calculated as the difference between F/F_0 at 10 min and F/F_0 at 0 min ($\Delta F/F_0$). Summarized data (mean ± SEM, B) showing the averaged value of $\Delta F/F_0$ in PASMCs from Nor (n = 120 cells), Nor + TMP (n = 96 cells), Hyp (n = 133 cells), and Hyp + TMP (n = 97 cells) groups. *P < .05, significantly different from Nor (without TMP treatment), #P < .05, significantly different from Hyp (without TMP treatment). (c) Representative records (A) and summarized data (mean ± SEM, B) showing the basal $[Ca^{2+}]_i$, (ratio at 340/380 nm, F340/380 nm) in PASMCs isolated from normoxic control rats (Nor) or rats exposed to chronic hypoxia (10% O_2) with (+TMP) or without TMP treatment (n = 5 rats for each group). Nor, n = 121 cells; Nor + TMP, n = 148 cells; Hyp, n = 119 cells; and Hyp + TMP, n = 109 cells. *P < .05, significantly different from Nor (without TMP treatment); #P < .05, significantly different from Hyp (without TMP treatment). (d) Representative records (A) showing Fura-2 fluorescence quenched by $MnCl_2$ in PASMCS from Nor, Nor + TMP, Hyp and Hyp + TMP groups of rats. SOCE is calculated as the difference between F/F_0 at 10 min and F/F_0 at 0 min ($\Delta F/F_0$). Summarized data (mean ± SEM, B) showing the averaged value of $\Delta F/F_0$ in PASMCs from Nor (n = 141 cells), Nor + TMP (n = 18 cells), Hyp (n = 153 cells), and Hyp + TMP (n = 118 cells) rats (n = 5 rats for each group). *P < .05, significantly different from Nor (without TMP treatment), #P < .05, significantly different from Hyp (without TMP treatment)

FIGURE 6 TMP inhibits hypoxia-mediated up-regulation of TRPC1 and TRPC6 in pulmonary arteries (PAs) from rats with experimental pulmonary hypertension (PH). (a, b) RT-PCR analyses on TRPC1 (a) and TRPC6 (b) in PAs isolated from normoxic control rats (Nor) and chronically hypoxic rats (Hyp) with (100 mg·kg^{-1}·day^{-1}) or without (0 mg·kg^{-1}·day^{-1}) treatment with TMP ; ($n = 6$ in each group). *$P < .05$ versus Nor (without TMP treatment); #$P < .05$ versus Hyp (without TMP treatment). (c) Representative western blot images (A) and summarized data (mean ± SEM; $n = 6$ in each group) showing protein levels of TRPC1 (B) and TRPC6 (C) in PAs isolated from Nor and Hyp rats with (100 mg·kg^{-1}·day^{-1}) or without (0 mg·kg^{-1}·day^{-1}) TMP treatment. *$P < .05$, significantly different from Nor (without TMP treatment); #$P < .05$, significantly different from Hyp (without TMP treatment). (d) Representative western blot images (A) and summarized data (mean ± SEM; $n = 6$ in each group) showing protein levels of TRPC1 (B) and TRPC6 (C) in PAs isolated from normoxic control rats (Nor) and Sugen/hypoxia-induced PH (SuHx) rats with (100 mg·kg^{-1}·day^{-1}) or without (0 mg·kg^{-1}·day^{-1}) TMP treatment. *$P < .05$, significantly different from Nor (without TMP treatment); #$P < .05$, significantly different from SuHx (without TMP treatment). (e) Representative western blot images (A) and summarized data (mean ± SEM; $n = 6$ in each group) showing protein levels of TRPC1 (B) and TRPC6 (C) in PAs isolated from control rats (CTL) and monocrotaline-induced PH (MCT) rats with (100 mg·kg^{-1}·day^{-1}) or without (0 mg·kg^{-1}·day^{-1}) TMP treatment. *$P < .05$, significantly different from CTL (without TMP treatment); #$P < .05$, significantly different from MCT (without TMP treatment)

3.8 | TMP inhibits hypoxia-induced increase of TRPC1 and TRPC6 mRNA and protein levels in PASMCs exposed to hypoxia

As shown in Figure 7, prolonged hypoxia (4% O_2, 60 hr) increased TRPC1 and TRPC6 at both mRNA (Figure 7a,b) and protein (Figure 7c) levels. TMP treatment (6.25 μM) markedly inhibited the hypoxia-induced up-regulation of TRPC1 and TRPC6 at both mRNA and protein levels, while it did not affect TRPC1 and TRPC6 expressions in normoxic PASMCs. Moreover, our data further indicated that TMP treatment (6.25 μM) also markedly inhibited the hypoxia-induced up-regulation of HIF-1α protein in PASMCs (Figure 7d).

3.9 | TMP inhibits the hypoxia-induced proliferation and migration in PASMCs

We then determined the effects of TMP on hypoxia-induced proliferation and migration in rat PASMCs isolated from distal pulmonary artery. As shown in Figure 8, treatment of the cells with TMP inhibited the hypoxia-induced PASMCs proliferation (Figure 8a) and migration (Figure 8b) in a dose-dependent fashion; TMP, however, had no significant effect on PASMCs proliferation or migration under normoxic conditions. Furthermore, we did not see obvious cytotoxic effects on the viability of PASMCs (Figure 8c) with the doses of TMP used for the in vitro experiments.
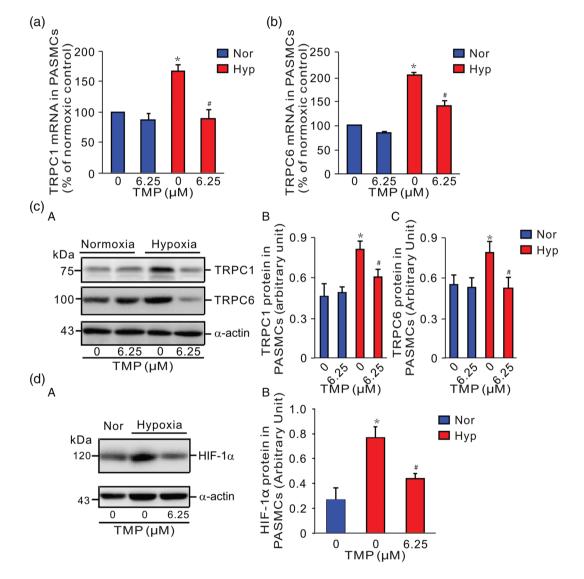

FIGURE 7 TMP inhibits hypoxia-induced up-regulation of TRPC1 and TRPC6 expression in PASMCs. We used primary cultured PASMCs prepared from distal pulmonary arteries of rats for this experiment. (a, b) RT-PCR analyses on TRPC1 (a) and TRPC6 (b) in PASMCs exposed to normoxia (Nor) and hypoxia (Hyp), with or without 6.25 μM of TMP (n = 5–6 rats in each group from which PASMCs are prepared). *$P < .05$, significantly different from Nor (without TMP treatment); #$P < .05$, significantly different from Hyp (without TMP treatment). (c) Representative western blot images (A) and summarized data (mean ± SEM; n = 5–6 in each group) showing protein levels of TRPC1 (B) and TRPC6 (C) in Nor-PASMCs and Hyp-PASMCs with or without 6.25 μM of TMP treatment. *$P < .05$, significantly different from Nor (without TMP treatment); #$P < .05$, significantly different from Hyp (without TMP treatment). (d) Representative western blot images (A) and summarized data (mean ± SEM; n = 5–6 in each group) showing protein level of HIF-1α (B) in Nor-PASMCs and Hyp-PASMCs (hypoxia) with or without 6.25 μM of TMP treatment. *$P < .05$, significantly different from Nor (without TMP treatment); #$P < .05$, significantly different from Hyp (without TMP treatment)
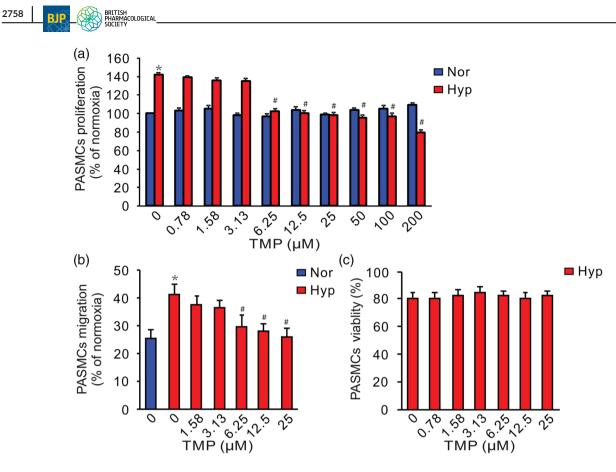
FIGURE 8 TMP inhibits hypoxia-induced PASMCs proliferation and migration. (a) Summarized data (mean ± SEM; n = 6 in each group) showing cell proliferation in normoxic control PASMCs (Nor) and PASMCs exposed to hypoxia (4% O_2 for 60 hr) in the absence (0 μM) and presence (0.78 to 200 μM) of TMP. (b) Summarized data (mean ± SEM; n = 6 in each group) showing cell migration in Nor-PASMCs and Hyp-PASMCs in the absence (0 μM) and presence (1.58 to 25 μM) of TMP. *P < .05, significantly different from Nor; #P < .05, significantly different from Hyp (without TMP treatment)

4 | RESULTS FROM THE RANDOMIZED CONTROLLED CLINICAL TRIAL

4.1 | Baseline data analysis

At baseline, patients were randomly assigned into either the TMP treatment group or the control group. There was no significant difference between the two groups in terms of demographic data (Table 1). Both groups consisted of patients with PAH and CTEPH. There were no significant differences in the distribution of PH classifications in the control and treatment groups (Table 1). At baseline before starting therapy, there were no significant differences in the primary outcomes of 6-min walking distance (6MWD) and heart rate recovery (HRR; Tables 2 and 3).

4.2 | TMP improves study outcomes (6MWD and HRR1) by 16 weeks

In the TMP group, 6MWD increased to 446 ± 80 m by 16 weeks (Table 2), while no significant increase was observed in the control group. The difference of 6MWD between the control and TMP groups only became significant at 16 weeks. The effect of TMP on

the 1-min heart rate recovery mirrored the changes in 6MWD (Table 3).

4.3 | Chronic TMP treatment improves secondary end points

At baseline, all subjects were categorized as either functional class II or III. By Week 16, the majority of the subjects had a function class of I or II (Table 4). Notably, the only significant changes with TMP treatment were in the Borg fatigue grading and the pulmonary arterial diameter (PAD). First, patients treated with TMP had a significant decrease in their Borg fatigue grading in the TMP treatment group, compared with the control group. However, although significant changes are shown in PAD among the groups, the differences were more likely present among different time points of treatment, but not between control and TMP treatment. Besides, no significant changes were observed in the other parameters. TMP decreased RVSP at the end of the study, while the control group showed a trend towards decrease by 8-weeks and had no further change at 16-weeks. All patients had a decrease in echocardiographic measurement of RA diameter (RAD) by 16 week, and there was no change in LVEF in either group. The ratio of PAD to aortic diameter increased in the

TABLE 1 Basic demographics of patients in the clinical study

Variable	Control	TMP
Number of patients	N = 12	N = 24
Age (years)	43 ± 19	43 ± 17
Gender (male : female)	7:5	17:7
Height (cm)	162 ± 7	159 ± 8
Weight (kg)	55 ± 8	55 ± 15
Body mass index (kg·m^{-2})	21 ± 3	21 ± 4
Pulmonary hypertension diagnosis		
PAH	6	14
CTEPH	6	10
Heart rate (bpm)	84 ± 8	83 ± 11
Respiratory rate (counts·min^{-1})	21 ± 1	21 ± 1
Serum creatinine (μM)	79 ± 17	78 ± 17
Right heart catheterization		
Pulmonary arterial systolic pressure, PASP (mmHg)	80 ± 21	82 ± 26
Pulmonary artery diastolic pressure, PADP (mmHg)	40 ± 14	37 ± 13
Mean pulmonary arterial pressure, mPAP (mmHg)	55 ± 16	52 ± 16
Pulmonary arterial wedge pressure, PAWP (mmHg)	7 ± 3	6 ± 6
Cardiac output, CO (L·min^{-1})	4.8 ± 1.9	3.8 ± 1.6
Cardiac index, CI [L/(min·m^{-2})]	21 ± 3	21 ± 4

TMP group (1.7 vs. 1.5) and the control group (1.6 vs. 1.5), but no significant difference was found between the TMP treatment group and the control group. There was a non-significant reduction in the number of small pericardial effusions in the TMP-treated group. Changes of secondary efficacy index between the two groups did not reach statistical significance.

4.4 | Safety end points

During the 16 weeks of observation, all patients had no significant fluctuation in BP. ALT levels were within the normal range in both groups; although the total bilirubin content at Week 16 appeared to be significantly different between the two groups, the values were within the normal range. All other indices were within the normal range, and no statistical difference found between before and after treatment (Table 1).

4.5 | Adverse events

No serious adverse effect was observed, and no drug withdrawal was related to adverse reactions. In patients experienced with mild adverse drug reactions (n = 2), a reduction of drug dosage and the symptom-specific treatment would resolve the symptoms, which indicated that the mild adverse drug reaction might not be related to TMP.

TABLE 2 TMP significantly increased the 6MWD by week 16 and there was no change in the control group

	6MWD			Change of 6MWD from baseline		
Visits	Control	TMP	P^a	Control	TMP	P^b
Baseline	367 ± 88	364 ± 89	.9			
Week 4	382 ± 81	397 ± 88	.6	14 ± 30	34 ± 24	.05
Week 8	388 ± 93	420 ± 83	.3	21 ± 47	56 ± 36	.02
Week 12	379 ± 95	427 ± 82	.1	12 ± 56	63 ± 40	.003
Week 16	385 ± 83	446 ± 80	.04	18 ± 49	82 ± 40	.001

Note. The data presented are mean ± SD. P^a and P^b are the results of a pairwise comparison between experimental (TMP) group and control group.

TABLE 3 TMP significantly improved the mean value of heart rate recovery at 1 min of rest (HRR1) at Week 16

	HRR1			Change of HHR1 from baseline		
Visits	Control	TMP	P^a	Control	TMP	P^b
Baseline	12.0 ± 6.1	10.1 ± 8.6	.5			
Week 4	13.7 ± 5.8	13.9 ± 10.0	.9	1.7 ± 3.9	3.8 ± 8.7	.4
Week 8	12.2 ± 4.7	14.7 ± 8.4	.4	0.2 ± 5.7	4.6 ± 6.3	.05
Week 12	11.9 ± 5.6	15.8 ± 7.9	.1	−0.1 ± 8.2	5.7 ± 5.4	.02
Week 16	13.0 ± 5.6	18.8 ± 7.8	.03	1.0 ± 4.2	6.4 ± 7.7	.001

Note. There were no significant changes in HRR1 in the control group (P = .9). The data presented are mean ± SD. P^a and P^b are the results of a pairwise comparison between TMP group and control group.

TABLE 4 TMP had significant effects on a few secondary outcome parameters

Variable	Baseline		Week 8		Week 16		P-values of comparison among groups
	Control	TMP	Control	TMP	Control	TMP	
Functional class							.6343
Class I	0	0	1	0	1	1	
Class II	6	15	8	16	8	17	
Class III	6	9	3	8	3	3	
Borg dyspnoea score	1.5 ± 1.8	1.7 ± 1.6	1.4 ± 1.6	0.9 ± 1.0	1.6 ± 1.6	0.7 ± 0.9	.005
Borg fatigue grading	3.9 ± 2.6	3.6 ± 1.9	4.7 ± 3.6	4.2 ± 3.4	3.5 ± 2.4	2.8 ± 1.7	.042
MLHFQ	49.6 ± 26.2	47.4 ± 18.5	40.1 ± 21.9	37.2 ± 19.1	36.0 ± 21.5	37.6 ± 20.7	.429
NT-proBNP	1,457 ± 1,049	1,654 ± 1,617	1,258 ± 992	1,219 ± 933	1,703 ± 990	1,115 ± 829	.993
cTnI ($\mu g \cdot L^{-1}$)	0.01 ± 0.01	0.02 ± 0.02	0.10 ± 0.29	0.01 ± 0.01	0.02 ± 0.01	0.02 ± 0.02	.651
RVSP (mmHg)	90 ± 27	89 ± 25	81 ± 22	76 ± 23	83 ± 27	73 ± 22	.324
RAD (mm)	44 ± 6	47 ± 11	40 ± 6	45 ± 11	41 ± 5	44 ± 10	.205
LVEF (%)	74 ± 8	72 ± 9	72 ± 6	71 ± 9	75 ± 6	72 ± 7	.399
Blood uric acid levels (μM)	628 ± 113	571 ± 97	550 ± 174	533 ± 126	502 ± 121	472 ± 147	.132
Pericardial effusion (none: small)	10: 2	17: 7	11: 1	19: 5	11: 1	23: 1	.4287
PAD (mm)	37 ± 9	38 ± 6	36 ± 3	38 ± 5	40 ± 4	41 ± 6	.006
AD (mm)	25 ± 3	25 ± 4	25 ± 3	24 ± 2	25 ± 4	23 ± 2	.857

Note. The data presented are mean ± *SD* or number of cases (%).
Abbreviations: AD, aortic diameter (mm); cTnI, cardiac troponin I ($\mu g \cdot L^{-1}$); LVEF, left ventricular ejection fraction (%); MLHFQ, the quality of life score of Minnesota heart failure; NT-proBNP, N-terminal pro-brain natriuretic peptide ($ng \cdot L^{-1}$); PAD, pulmonary artery diameter (mm); RAD, right atrium diameter (mm); RVSP, right ventricular systolic pressure (mmHg); WHO, WHO functional class.

TABLE 5 Mean changes in safety index from baseline to Week 16

Security index	Baseline			Week 16		
	Control	TMP	P	Control	TMP	P
BP (mmHg)						
Systolic BP	115 ± 8	109 ± 14	.165	116 ± 8	110 ± 11	.101
Diastolic BP	74 ± 7	69 ± 10	.095	75 ± 8	70 ± 8	.082
Alanine aminotransferase (U/L)	32.71 ± 11.81	22.80 ± 15.40	.059	29.47 ± 19.56	26.24 ± 13.23	.562
Total bilirubin (μM)	17.08 ± 6.99	12.03 ± 8.93	.097	17.83 ± 6.75	10.46 ± 6.79	.004
Urea nitrogen (μM)	4.86 ± 1.10	4.88 ± 1.88	.965	4.88 ± 2.04	5.21 ± 2.42	.686
Serum creatinine (μM)	79.31 ± 17.15	77.95 ± 16.64	.820	77.72 ± 17.24	82.18 ± 21.86	.542
Prothrombin time (s)	15.5 ± 1.6	15.0 ± 1.6	.488	17.1 ± 3.2	16.3 ± 2.2	.358

Note. The data presented are mean ± *SD* or number of cases (%).

5 | DISCUSSION

In this study, our results demonstrated that TMP is a potential new therapeutic agent for PH. In PAH and CTEPH patients, 16 weeks of TMP treatment effectively increased the average 6-min walk distance (6MWD). In three well-established PH rat models, TMP treatment inhibited and reversed PH-related increases in RVSP, RV hypertrophy, and pulmonary vascular remodelling. Our present results are similar to the findings in a much earlier publication (Cai & Barer, 1989). Like most traditional Chinese medicines, the pharmacological and molecular target of TMP is largely unknown. Our in vitro experiment results

suggested that TMP decreases proliferation and migration of PASMCs by targeting the TRPC-SOCE-$[Ca^{2+}]_i$ signalling axis. Based on its long history of safe usage, high efficacy, low expense, few adverse effects and easy oral administration (Bai et al., 2014; Chen & Chen, 1992; Fu et al., 2012; Shaw et al., 2013; Wang, Yang, et al., 2013; Zeng et al., 2013; Zhu et al., 2009), and significant effects from both in vivo and in vitro studies, TMP is potentially an ideal and affordable drug for the treatment of PAH.

Chronic hypoxia is an important trigger for the increase in $[Ca^{2+}]_i$ in PASMCs, which results in pulmonary vasoconstriction, stimulates PASMC proliferation causing distal PA thickening and remodelling,

and leads ultimately to the development of PH (Hou et al., 2013; Mandegar et al., 2004; Yamamura, Yamamura, & Yuan, 2013; Zhang, Liu, Yang, & Lin, 2010). We have previously observed that the elevated $[Ca^{2+}]_i$ in hypoxic PASMCs is largely mediated by enhanced SOCE through SOCC (Shimoda, Wang, & Sylvester, 2006). The hypoxia-enhanced SOCE is mediated by the hypoxic up-regulation of canonical TRPC1 and TRPC6 ion channels, the main components of SOCC in PASMCs (Hou et al., 2013; Li et al., 2013; Malczyk et al., 2013; Wang et al., 2013; Wang et al., 2013; Wang et al., 2014; Xia et al., 2014; Zhang et al., 2013). The data from this study further indicate that the therapeutic effect of TMP is due, at least partly, to its down-regulation of TRPC channel expression and inhibition of intracellular Ca^{2+} signalling in PASMCs. Our data also indicate that TMP can attenuate the hypoxia-induced up-regulation of TRPC channels, enhancement of SOCE, and increases in the basal $[Ca^{2+}]_i$ in PASMCs based on the in vivo and in vitro experiments.

Previous studies have demonstrated that TMP suppresses cell proliferation and blocks the synthesis of Type I collagen, acting a reliable vasodilator that principally targets the vascular smooth muscle and right ventricle (Lin et al., 2006; Nie, Ran, & Zeng, 2012; Yu, Wang, & Sun, 2012; Zhang et al., 2009). In the current study, we also found that TMP attenuates the hypoxia-mediated accumulation of HIF-1α proteins; these data suggest that TMP may prevent and reverse PH via modulation of HIF-1α protein level and HIF-1 associated signalling pathways. HIF-1α is a highly conserved transcription factor that is present in almost all metazoan cell types. It contributes to the pathogenesis of numerous pulmonary diseases, including PH associated with chronic hypoxia and hypoxemia (Wang et al., 2006). In PASMCs, HIF-1α can induce abnormal membrane ion channel homeostasis, lead to membrane depolarization caused by reduced K^+ channel expression/activity (Bonnet et al., 2006), and enhance the extracellular Ca^{2+} influx through the TRPC/SOCC channels (Wang et al., 2006). Our data indicated that (a) TMP markedly attenuated the hypoxia-induced up-regulation of TRPC, enhancement of SOCE, and increase of the basal $[Ca^{2+}]_i$ in PASMCs from hypoxic rats and (b) TMP could lead to a reduction in HIF-1α that could be the molecular basis of TMP-induced anti-proliferation and anti-migration effect on distal PASMCs.

Regarding to the acute vasodilator effect of TMP, we found that only inhibition of K_{Ca} channels with TEA attenuated TMP-mediated vasodilation in isolated rings of distal PA, whereas inhibition of K_{ATP} (with glibenglamide), K_{IR} (with Ba^{2+}), and K_V (with 4-AP) channels failed to affect the TMP-mediated pulmonary vasodilation. These observations suggest that activation of the large conductance K_{Ca} channels in PASMCs is an important mechanism by which TMP causes pulmonary vasodilation. Moreover, our data from echocardiographic analysis also showed protective effect of TMP on the right heart function. TMP treatment partly reversed the dysregulated right heart function, reflected by parameters of fractional area change (FAC), tricuspid annular plane systolic excursion (TAPSE), RV end-diastolic free-wall thickness (RVEDWT), RV end-diastolic diameter (RVEDD), and pulmonary acceleration time/pulmonary ejection time (PAT/PET).

Based on the preclinical in vivo and in vitro studies, we also conducted a small-scale clinical trial that enrolled 24 PH patients and 12 control subjects. Results showed a beneficial effect of TMP after 16 weeks of treatment. In this trial, we demonstrated that patients who received TMP therapy had an improvement in their 6MWD and heart rate recovery at 1 min. TMP had no significant effect on safety end points of BP, alanine aminotransferase with 16 weeks of therapy. This pilot trial also suggests a restoration of the outcome parameters by TMP, including the Borg dyspnoea grading and PAD. Although, as a limitation, this study was not blinded among investigators and patients, the results from this small clinical study provide important evidence indicating that TMP is potentially an efficient and safe treatment for patients with chronic PH. A large clinical study is needed to further elucidate the clinical safety and efficacy of TMP in the treatment of PH.

In summary, TMP is potentially an effective and safe treatment for pulmonary hypertension based on its acute vasodilator effect on distal pulmonary arteries and its anti-proliferative effect on PASMCs. The therapeutic effects of TMP in in vitro and in vivo experiments were also reproduced in a small-scale clinical trial in which TMP treatment for 13 weeks significantly improved 6MWD and right heart function. TMP is a valuable candidate compound for the treatment of PH, based on its long history of clinical use, low cost, easy oral administration, and high efficiency, with few adverse effects.

AUTHOR CONTRIBUTIONS

J.W. initiated and designed the project, analysed the data from both basic and clinical studies and wrote the manuscript. W.L. and N.S.Z. contributed to the design of the project. Y.C. performed the

animal experiments, analysed the data, and contributed to the design of the clinical trial. X.C. and S.L. performed the animal and functional experiments and analysed the data. M.L. and X.D. performed the clinical study and analysed the data. K.Y. contributed to the editing and revision of the manuscript and provided critical suggestions for the experimental design of the basic study. X.W., Q.Z., J.C., and J.L. contributed to the molecular experiments. M.K., J.Z., G.Z., and C. Hou performed the animal experiments. W.H., C.L., C. Hong, and N.F.Z. contributed to the clinical trial. H.T. provided consultation and advice on the functional and molecular experiments. J.X.J.Y. and R.R.V. provided consultation and advice on the project and edited the manuscript. A.A.D., F.R., S.M.B., J.G.N.G., and A.M. provided consultation and advice on the project.

CONFLICT OF INTEREST

The authors declare no conflicts of interest.

DECLARATION OF TRANSPARENCY AND SCIENTIFIC RIGOUR

This Declaration acknowledges that this paper adheres to the principles for transparent reporting and scientific rigour of preclinical research as stated in the BJP guidelines for Design & Analysis, Immunoblotting and Immunochemistry, and Animal Experimentation, and as recommended by funding agencies, publishers and other organisations engaged with supporting research.

ORCID

Wenju Lu https://orcid.org/0000-0002-5035-9287

Kai Yang https://orcid.org/0000-0003-3044-2240

Jian Wang https://orcid.org/0000-0002-1278-256X

REFERENCES

Alexander, S. P. H., Fabbro, D., Kelly, E., Mathie, A., Peters, J. A., Veale, E. L., … CGTP Collaborators. (2019). THE CONCISE GUIDE TO PHARMACOLOGY 2019/20: Enzymes. *British Journal of Pharmacology*, 176, S297–S396. https://doi.org/10.1111/bph.14752

Alexander, S. P. H., Mathie, A., Peters, J. A., Veale, E. L., Striessnig, J., Kelly, E., … CGTP Collaborators. (2019). THE CONCISE GUIDE TO PHARMACOLOGY 2019/20: Ion channels. *British Journal of Pharmacology*, 176, S142–S228. https://doi.org/10.1111/bph.14749

Alexander, S. P. H., Roberts, R. E., Broughton, B. R. S., Sobey, C. G., George, C. H., Stanford, S. C., … Ahluwalia, A. (2018). Goals and practicalities of immunoblotting and immunohistochemistry: A guide for submission to the *British Journal of Pharmacology*. *British Journal of Pharmacology*, 175(3), 407–411. https://doi.org/10.1111/bph.14112

Bai, X. Y., Zhang, P., Yang, Q., Liu, X. C., Wang, J., Tong, Y. L., … He, G.-W. (2014). Suxiao jiuxin pill induces potent relaxation and inhibition on contraction in human artery and the mechanism. *Evidence-Based Complementary and Alternative Medicine*, 2014, 956924. https://doi.org/10.1155/2014/956924

Benza, R., Mathai, S., & Nathan, S. D. (2017). sGC stimulators: Evidence for riociguat beyond groups 1 and 4 pulmonary hypertension. *Respiratory Medicine*, 122(Suppl 1), S28–S34. https://doi.org/10.1016/j.rmed.2016.11.010

Benza, R. L., Miller, D. P., Gomberg-Maitland, M., Frantz, R. P., Foreman, A. J., Coffey, C. S., … McGoon, M. (2010). Predicting survival in pulmonary arterial hypertension: Insights from the Registry to Evaluate Early and Long-Term Pulmonary Arterial Hypertension Disease Management (REVEAL). *Circulation*, 122(2), 164–172. https://doi.org/10.1161/CIRCULATIONAHA.109.898122

Bonnet, S., Michelakis, E. D., Porter, C. J., Andrade-Navarro, M. A., Thebaud, B., Bonnet, S., … Archer, S. L. (2006). An abnormal mitochondrial-hypoxia inducible factor-1α-K$_v$ channel pathway disrupts oxygen sensing and triggers pulmonary arterial hypertension in fawn hooded rats: Similarities to human pulmonary arterial hypertension. *Circulation*, 113(22), 2630–2641. https://doi.org/10.1161/CIRCULATIONAHA.105.609008

Cai, Y. N., & Barer, G. R. (1989). Effect of ligustrazine on pulmonary vascular changes induced by chronic hypoxia in rats. *Clinical Science (London, England)*, 77(5), 515–520. https://doi.org/10.1042/cs0770515

Chen, K. J., & Chen, K. (1992). Ischemic stroke treated with Ligusticum chuanxiong. *Chinese Medical Journal*, 105(10), 870–873.

Clements, P. J., Tan, M., McLaughlin, V. V., Oudiz, R. J., Tapson, V. F., Channick, R. N., … Pulmonary Arterial Hypertension Quality Enhancement Research Initiative (PAH-QuERI) Investigators. (2012). The pulmonary arterial hypertension quality enhancement research initiative: comparison of patients with idiopathic PAH to patients with systemic sclerosis-associated PAH. *Annals of the Rheumatic Diseases*, 71(2), 249–252. https://doi.org/10.1136/annrheumdis-2011-200265

Coyle, K., Coyle, D., Blouin, J., Lee, K., Jabr, M. F., Tran, K., … Innes, M. (2016). Cost effectiveness of first-line oral therapies for pulmonary arterial hypertension: A modelling study. *PharmacoEconomics*, 34(5), 509–520. https://doi.org/10.1007/s40273-015-0366-8

Curtis, M. J., Alexander, S., Cirino, G., Docherty, J. R., George, C. H., Giembycz, M. A., … Ahluwalia, A. (2018). Experimental design and analysis and their reporting II: Updated and simplified guidance for authors and peer reviewers. *British Journal of Pharmacology*, 175(7), 987–993. https://doi.org/10.1111/bph.14153

Divakaran, S., & Loscalzo, J. (2017). The role of nitroglycerin and other nitrogen oxides in cardiovascular therapeutics. *Journal of the American College of Cardiology*, 70(19), 2393–2410. https://doi.org/10.1016/j.jacc.2017.09.1064

Fernandez, R. A., Wan, J., Song, S., Smith, K. A., Gu, Y., Tauseef, M., … Yuan, J. X. (2015). Upregulated expression of STIM2, TRPC6, and Orai2 contributes to the transition of pulmonary arterial smooth muscle cells from a contractile to proliferative phenotype. *American Journal of Physiology. Cell Physiology*, 308(8), C581–C593. https://doi.org/10.1152/ajpcell.00202.2014

Frumkin, L. R. (2012). The pharmacological treatment of pulmonary arterial hypertension. *Pharmacological Reviews*, 64(3), 583–620. https://doi.org/10.1124/pr.111.005587

Fu, C., Yu, L., Zou, Y., Cao, K., Zhao, J., Gong, H., … Li, T. (2012). Efficacy of chuanxiong ding tong herbal formula granule in the treatment and prophylactic of migraine patients: A randomized, double-blind, multicenter, placebo-controlled trial. *Evidence-Based Complementary and Alternative Medicine*, 2012, 967968. https://doi.org/10.1155/2012/967968

Guo, M., Liu, Y., & Shi, D. (2016). Cardiovascular actions and therapeutic potential of tetramethylpyrazine (active component isolated from Rhizoma Chuanxiong): Roles and mechanisms. *BioMed Research International*, 2016, 2430329. https://doi.org/10.1155/2016/2430329

Hao, Y. J., Jiang, X., Zhou, W., Wang, Y., Gao, L., Li, G. T., … Zhang, Z.-L. (2014). Connective tissue disease-associated pulmonary arterial hypertension in Chinese patients. *The European Respiratory Journal*, 44(4), 963–972. https://doi.org/10.1183/09031936.00182813

Harding, S. D., Sharman, J. L., Faccenda, E., Southan, C., Pawson, A. J., Ireland, S., … NC-IUPHAR. (2018). The IUPHAR/BPS Guide to PHARMACOLOGY in 2018: updates and expansion to encompass the new guide to IMMUNOPHARMACOLOGY. *Nucleic Acids Res.*, 46, D1091–D1106. https://doi.org/10.1093/nar/gkx1121

Hou, X., Chen, J., Luo, Y., Liu, F., Xu, G., & Gao, Y. (2013). Silencing of STIM1 attenuates hypoxia-induced PASMCs proliferation via inhibition of the SOC/Ca^{2+}/NFAT pathway. *Respiratory Research*, *14*, 2. https://doi.org/10.1186/1465-9921-14-2

Kane, G. C., Maradit-Kremers, H., Slusser, J. P., Scott, C. G., Frantz, R. P., & McGoon, M. D. (2011). Integration of clinical and hemodynamic parameters in the prediction of long-term survival in patients with pulmonary arterial hypertension. *Chest*, *139*(6), 1285–1293. https://doi.org/10.1378/chest.10-1293

Karaki, H., Ozaki, H., Hori, M., Mitsui-Saito, M., Amano, K., Harada, K., ... Sato, K. (1997). Calcium movements, distribution, and functions in smooth muscle. *Pharmacological Reviews*, *49*(2), 157–230.

Kilkenny, C., Browne, W., Cuthill, I. C., Emerson, M., & Altman, D. G. (2010). Animal research: Reporting in vivo experiments: The ARRIVE guidelines. *British Journal of Pharmacology*, *160*, 1577–1579.

Kuhr, F. K., Smith, K. A., Song, M. Y., Levitan, I., & Yuan, J. X. (2012). New mechanisms of pulmonary arterial hypertension: role of Ca^{2+} signaling. *American Journal of Physiology. Heart and Circulatory Physiology*, *302*(8), H1546–H1562. https://doi.org/10.1152/ajpheart.00944.2011

Li, X., Lu, W., Fu, X., Zhang, Y., Yang, K., Zhong, N., ... Wang, J. (2013). BMP4 increases canonical transient receptor potential protein expression by activating p38 MAPK and ERK1/2 signaling pathways in pulmonary arterial smooth muscle cells. *American Journal of Respiratory Cell and Molecular Biology*, *49*(2), 212–220. https://doi.org/10.1165/rcmb.2012-0051OC

Lin, M. J., Leung, G. P., Zhang, W. M., Yang, X. R., Yip, K. P., Tse, C. M., & Sham, J. S. (2004). Chronic hypoxia-induced upregulation of store-operated and receptor-operated Ca^{2+} channels in pulmonary arterial smooth muscle cells: A novel mechanism of hypoxic pulmonary hypertension. *Circulation Research*, *95*(5), 496–505. https://doi.org/10.1161/01.RES.0000138952.16382.ad

Lin, Y. Z., Xu, C. X., Deng, Y. L., Chen, L., Huang, H., & Du, J. (2006). Effects of tetramethylpyrazine on fibrosis of atrial tissue and atrial fibrillation in a canine model of congestive heart failure induced by ventricular tachypacing. *Zhong Xi Yi Jie He Xue Bao*, *4*(1), 35–38. https://doi.org/10.3736/jcim20060110

Lu, W., Ran, P., Zhang, D., Peng, G., Li, B., Zhong, N., & Wang, J. (2010). Sildenafil inhibits chronically hypoxic upregulation of canonical transient receptor potential expression in rat pulmonary arterial smooth muscle. *American Journal of Physiology. Cell Physiology*, *298*(1), C114–C123. https://doi.org/10.1152/ajpcell.00629.2008

Lu, W., Wang, J., Peng, G., Shimoda, L. A., & Sylvester, J. T. (2009). Knockdown of stromal interaction molecule 1 attenuates store-operated Ca^{2+} entry and Ca^{2+} responses to acute hypoxia in pulmonary arterial smooth muscle. *American Journal of Physiology. Lung Cellular and Molecular Physiology*, *297*(1), L17–L25. https://doi.org/10.1152/ajplung.00063.2009

Lu, W., Wang, J., Shimoda, L. A., & Sylvester, J. T. (2008). Differences in STIM1 and TRPC expression in proximal and distal pulmonary arterial smooth muscle are associated with differences in Ca^{2+} responses to hypoxia. *American Journal of Physiology. Lung Cellular and Molecular Physiology*, *295*(1), L104–L113. https://doi.org/10.1152/ajplung.00058.2008

Malczyk, M., Veith, C., Fuchs, B., Hofmann, K., Storch, U., Schermuly, R. T., ... Weissmann, N. (2013). Classical transient receptor potential channel 1 in hypoxia-induced pulmonary hypertension. *American Journal of Respiratory and Critical Care Medicine*, *188*(12), 1451–1459. https://doi.org/10.1164/rccm.201307-1252OC

Mandegar, M., Fung, Y. C., Huang, W., Remillard, C. V., Rubin, L. J., & Yuan, J. X. (2004). Cellular and molecular mechanisms of pulmonary vascular remodeling: Role in the development of pulmonary hypertension. *Microvascular Research*, *68*(2), 75–103. https://doi.org/10.1016/j.mvr.2004.06.001

Nie, H., Ran, X., & Zeng, Z. (2012). Effect of tetramethylpyrazine on Nogo gene regulation of the proliferation in cardiac fibroblast. *Sichuan Da Xue Xue Bao. Yi Xue Ban*, *43*(6), 843–846.

Oddoy, A., Bee, D., Emery, C., & Barer, G. (1991). Effects of ligustrazine on the pressure/flow relationship in isolated perfused rat lungs. *The European Respiratory Journal*, *4*(10), 1223–1227.

Peng, W., Hucks, D., Priest, R. M., Kan, Y. M., & Ward, J. P. (1996). Ligustrazine-induced endothelium-dependent relaxation in pulmonary arteries via an NO-mediated and exogenous L-arginine-dependent mechanism. *British Journal of Pharmacology*, *119*(5), 1063–1071. https://doi.org/10.1111/j.1476-5381.1996.tb15778.x

Pfaffl, M. W. (2001). A new mathematical model for relative quantification in real-time RT-PCR. *Nucleic Acids Research*, *29*(9), e45. https://doi.org/10.1093/nar/29.9.e45

Pullamsetti, S. S., Schermuly, R., Ghofrani, A., Weissmann, N., Grimminger, F., & Seeger, W. (2014). Novel and emerging therapies for pulmonary hypertension. *American Journal of Respiratory and Critical Care Medicine*, *189*(4), 394–400. https://doi.org/10.1164/rccm.201308-1543PP

Putnam, L. R., Tsao, K., Morini, F., Lally, P. A., Miller, C. C., Lally, K. P., ... Congenital Diaphragmatic Hernia Study Group. (2016). Evaluation of variability in inhaled nitric oxide use and pulmonary hypertension in patients with congenital diaphragmatic hernia. *JAMA Pediatrics*, *170*(12), 1188–1194. https://doi.org/10.1001/jamapediatrics.2016.2023

Robinson, J. C., Pugliese, S. C., Fox, D. L., & Badesch, D. B. (2016). Anticoagulation in pulmonary arterial hypertension. *Current Hypertension Reports*, *18*(6), 47. https://doi.org/10.1007/s11906-016-0657-2

Shaw, L. H., Chen, W. M., & Tsai, T. H. (2013). Identification of multiple ingredients for a traditional Chinese medicine preparation (bu-yang-huan-wu-tang) by liquid chromatography coupled with tandem mass spectrometry. *Molecules*, *18*(9), 11281–11298. https://doi.org/10.3390/molecules180911281

Shimoda, L. A., Sham, J. S., & Sylvester, J. T. (2000). Altered pulmonary vasoreactivity in the chronically hypoxic lung. *Physiological Research*, *49*(5), 549–560.

Shimoda, L. A., Wang, J., & Sylvester, J. T. (2006). Ca^{2+} channels and chronic hypoxia. *Microcirculation*, *13*(8), 657–670. https://doi.org/10.1080/10739680600930305

Thenappan, T., Glassner, C., & Gomberg-Maitland, M. (2012). Validation of the pulmonary hypertension connection equation for survival prediction in pulmonary arterial hypertension. *Chest*, *141*(3), 642–650. https://doi.org/10.1378/chest.11-0969

Wang, J., Chen, Y., Lin, C., Jia, J., Tian, L., Yang, K., ... Lu, W. (2014). Effects of chronic exposure to cigarette smoke on canonical transient receptor potential expression in rat pulmonary arterial smooth muscle. *American Journal of Physiology. Cell Physiology*, *306*(4), C364–C373. https://doi.org/10.1152/ajpcell.00048.2013

Wang, J., Jiang, Q., Wan, L., Yang, K., Zhang, Y., Chen, Y., ... Lu, W. (2013). Sodium tanshinone IIA sulfonate inhibits canonical transient receptor potential expression in pulmonary arterial smooth muscle from pulmonary hypertensive rats. *American Journal of Respiratory Cell and Molecular Biology*, *48*(1), 125–134. https://doi.org/10.1165/rcmb.2012-0071OC

Wang, J., Shimoda, L. A., & Sylvester, J. T. (2004). Capacitative calcium entry and TRPC channel proteins are expressed in rat distal pulmonary arterial smooth muscle. *American Journal of Physiology. Lung Cellular and Molecular Physiology*, *286*(4), L848–L858. https://doi.org/10.1152/ajplung.00319.2003

Wang, J., Shimoda, L. A., Weigand, L., Wang, W., Sun, D., & Sylvester, J. T. (2005). Acute hypoxia increases intracellular [Ca^{2+}] in pulmonary arterial smooth muscle by enhancing capacitative Ca^{2+} entry. *American Journal of Physiology. Lung Cellular and Molecular Physiology*, *288*(6), L1059–L1069. https://doi.org/10.1152/ajplung.00448.2004

Wang, J., Weigand, L., Lu, W., Sylvester, J. T., Semenza, G. L., & Shimoda, L. A. (2006). Hypoxia inducible factor 1 mediates hypoxia-induced TRPC expression and elevated intracellular Ca^{2+} in pulmonary arterial smooth muscle cells. *Circulation Research*, 98(12), 1528–1537. https://doi.org/10.1161/01.RES.0000227551.68124.98

Wang, J., Yang, K., Xu, L., Zhang, Y., Lai, N., Jiang, H., … Lu, W. (2013). Sildenafil inhibits hypoxia-induced transient receptor potential canonical protein expression in pulmonary arterial smooth muscle via cGMP-PKG-PPARγ axis. *American Journal of Respiratory Cell and Molecular Biology*, 49(2), 231–240. https://doi.org/10.1165/rcmb.2012-0185OC

Wang, L., Zhang, J., Hong, Y., Feng, Y., Chen, M., & Wang, Y. (2013). Phytochemical and pharmacological review of Da Chuanxiong formula: A famous herb pair composed of Chuanxiong Rhizoma and Gastrodiae Rhizoma for headache. *Evidence-Based Complementary and Alternative Medicine*, 2013, 425369.

Ward, J. P., Robertson, T. P., & Aaronson, P. I. (2005). Capacitative calcium entry: A central role in hypoxic pulmonary vasoconstriction? *American Journal of Physiology. Lung Cellular and Molecular Physiology*, 289(1), L2–L4. https://doi.org/10.1152/ajplung.00101.2005

Weigand, L., Foxson, J., Wang, J., Shimoda, L. A., & Sylvester, J. T. (2005). Inhibition of hypoxic pulmonary vasoconstriction by antagonists of store-operated Ca^{2+} and nonselective cation channels. *American Journal of Physiology. Lung Cellular and Molecular Physiology*, 289(1), L5–L13. https://doi.org/10.1152/ajplung.00044.2005

Wryobeck, J. M., Lippo, G., McLaughlin, V., Riba, M., & Rubenfire, M. (2007). Psychosocial aspects of pulmonary hypertension: A review. *Psychosomatics*, 48(6), 467–475. https://doi.org/10.1176/appi.psy.48.6.467

Xia, Y., Yang, X. R., Fu, Z., Paudel, O., Abramowitz, J., Birnbaumer, L., & Sham, J. S. (2014). Classical transient receptor potential 1 and 6 contribute to hypoxic pulmonary hypertension through differential regulation of pulmonary vascular functions. *Hypertension*, 63(1), 173–180. https://doi.org/10.1161/HYPERTENSIONAHA.113.01902

Yamamura, A., Yamamura, H., & Yuan, J. X. (2013). Enhanced Ca^{2+}-sensing receptor function in pulmonary hypertension. *Yakugaku Zasshi*, 133(12), 1351–1359. https://doi.org/10.1248/yakushi.13-00228-3

Yoo, H. Y., Zeifman, A., Ko, E. A., Smith, K. A., Chen, J., Machado, R. F., … Yuan, J. X. (2013). Optimization of isolated perfused/ventilated mouse lung to study hypoxic pulmonary vasoconstriction. *Pulm Circ*, 3(2), 396–405. https://doi.org/10.4103/2045-8932.114776

Yu, Y., Wang, S. R., & Sun, Y. K. (2012). Effects of ligustrazine on the mitochondrial structure and functions in the process myocardial hypertrophy. *Zhongguo Zhong Xi Yi Jie He Za Zhi*, 32(5), 661–665.

Zeng, M., Pan, L., Qi, S., Cao, Y., Zhu, H., Guo, L., & Zhou, J. (2013). Systematic review of recent advances in pharmacokinetics of four classical Chinese medicines used for the treatment of cerebrovascular disease. *Fitoterapia*, 88, 50–75. https://doi.org/10.1016/j.fitote.2013.04.006

Zhai, Z., Zhou, X., Zhang, S., Xie, W., Wan, J., Kuang, T., … Wang, C. (2017). The impact and financial burden of pulmonary arterial hypertension on patients and caregivers: Results from a national survey. *Medicine (Baltimore)*, 96(39), e6783. https://doi.org/10.1097/MD.0000000000006783

Zhang, D. M., Qin, Y., Lu, X. Y., Wu, A. M., Zhu, L. Q., Wang, S. R., & Jiang, L. D. (2009). Effects of tetramethylpyrazine on angiotensin II-induced proliferation and type I collagen synthesis of rat cardiac fibroblasts. *Zhong Xi Yi Jie He Xue Bao*, 7(3), 232–236. https://doi.org/10.3736/jcim20090307

Zhang, M. F., Liu, X. R., Yang, N., & Lin, M. J. (2010). TRPC6 mediates the enhancements of pulmonary arterial tone and intracellular Ca^{2+} concentration of pulmonary arterial smooth muscle cells in pulmonary hypertension rats. *Sheng Li Xue Bao*, 62(1), 55–62.

Zhang, Y., Lu, W., Yang, K., Xu, L., Lai, N., Tian, L., … Wang, J. (2013). Bone morphogenetic protein 2 decreases TRPC expression, store-operated Ca^{2+} entry, and basal $[Ca^{2+}]_i$ in rat distal pulmonary arterial smooth muscle cells. *American Journal of Physiology. Cell Physiology*, 304(9), C833–C843. https://doi.org/10.1152/ajpcell.00036.2012

Zhu, L. Q., Wang, S. R., & Qin, Y. (2009). Effects of huoxue injection on the adherence of human monocytes to endothelial cells and expression of vascular cell adhesion molecules. *Zhongguo Zhong Xi Yi Jie He Za Zhi*, 29(3), 238–241.

SUPPORTING INFORMATION

Additional supporting information may be found online in the Supporting Information section at the end of this article.